

M 2014

# **Effects of personal care products on rainbow trout (*Oncorhynchus mykiss*) hepatocytes**

MARIA LAURA AMBERGER

DISSERTAÇÃO DE MESTRADO APRESENTADA

AO INSTITUTO DE CIÊNCIAS BIOMÉDICAS ABEL SALAZAR

DA UNIVERSIDADE DO PORTO EM

TOXICOLOGIA E CONTAMINAÇÃO AMBIENTAIS



Maria Laura Amberger

**Effects of personal care products on rainbow trout  
(*Oncorhynchus mykiss*) hepatocytes**

Dissertação de Candidatura ao grau de Mestre em Toxicologia e Contaminação Ambientais submetida ao Instituto de Ciências Biomédicas de Abel Salazar da Universidade do Porto.

Orientador – Ketil Hylland

Categoria – Professor catedrático

Afiliação – Department of Biosciences, Faculty of Mathematics and Natural Sciences, University of Oslo, Norway.

Co-orientador – Lúcia Guilhermino

Categoria – Professora catedrática

Afiliação – Instituto de Ciências Biomédicas Abel Salazar (ICBAS) da Universidade do Porto, Departamento de Estudo de Populações, Laboratório de Ecotoxicologia; Centro Interdisciplinar de Investigação Marinha e Ambiental (CIIMAR), Grupo de Investigação em Ecotoxicologia, Ecologia do Stresse e Saúde Ambiental.



## Abstract

The presence of chemicals in the environment raises concerns in relation to their potential adverse effects on human and environmental health. Personal care products (PCPs) are used daily by a large part of the human population and have been increasingly found in the environment. They end up in surface waters mainly through domestic and industrial wastewater discharges. Despite their relatively low toxicity, these chemicals constitute a threat to the aquatic ecosystems, since they may accumulate in aquatic organisms and adsorb to suspended solids and sediments. Polycyclic musks are known to interfere with the multixenobiotic resistance (MXR) defense mechanism of cells and, together with diethyl phthalate (DEP), they impair the cellular structure and cell functions. In this context, the potential of the polycyclic musks tonalide (AHTN) and galaxolide (HHCB) and the phthalate ester DEP to cause toxicity in rainbow trout (*Oncorhynchus mykiss*) was assessed. Acute *in vitro* exposure of *O. mykiss* hepatocytes to single and binary mixtures of PCPs was performed. Cytotoxicity caused by single PCPs was evaluated through the application of the fluorescent probes alamar blue (AB), 5-carboxyfluorescein diacetate acetoxymethyl ester (CFDA-AM) and monochlorobimane (mBCI), which allows the measurement of the levels of cell mitochondrial activity, membrane integrity and oxidative stress, respectively. Furthermore, the potential of single and combined PCPs to inhibit the activity of ABC transporters in cells was evaluated. To better understand the toxicity of mixtures, comparisons between experimental results and concentration addition (CA) and independent action (IA) model predictions were done. PCPs caused cytotoxic effects on *O. mykiss* hepatocytes, namely a dose-dependent decrease of cellular mitochondrial activity and membrane integrity, and induction of oxidative stress. The lowest EC<sub>50</sub> values for PCPs corresponded to membrane integrity impairment:  $111.40 \times 10^{-6}$  M for AHTN,  $3.67 \times 10^{-6}$  M for HHCB and  $25.31 \times 10^{-3}$  M for DEP. In relation to oxidative stress, hepatocytes seem to cope with low concentrations of AHTN ( $0.02\text{--}23.3 \times 10^{-6}$  M), HHCB ( $0.02\text{--}2.3 \times 10^{-6}$  M) and DEP ( $2.3\text{--}20000 \times 10^{-6}$  M). However, impairment of the antioxidant defense system seems to occur at higher concentrations. Furthermore, hepatocytes exposed to single and binary mixtures of PCPs presented a dose-dependent decrease in cellular ABC transporter activity. Therefore, the tested compounds induced cytotoxic effects on rainbow trout hepatocytes and inhibited the MXR defense system of cells, consequently acting as chemosensitizers. HHCB was the most toxic compound for rainbow trout hepatocytes, followed by AHTN and DEP. Model predictions indicated toxicological interactions when the compounds were tested in binary mixtures, namely antagonism caused by the HHCB/DEP mixture. The effects of the AHTN/HHCB mixture revealed to be additive. In general, these findings highlight the importance of diagnosing

the presence of potential MXR inhibitors in the environment and the need of more research on the toxic effects caused by chemical mixtures. Aquatic organisms, including fish, become more susceptible to the potential adverse effects caused by exposure to xenobiotics if the MXR defense system is compromised, especially under exposure to chemicals able to cause synergistic effects.

## Resumo

A presença de substâncias químicas no ambiente gera preocupações devido aos seus potenciais efeitos negativos na saúde humana e ambiental. Os produtos de higiene e cuidado pessoal (PCPs) são usados diariamente por uma grande parte da população e, portanto, estão cada vez mais presentes no ambiente. Através de descargas de águas residuais domésticas e industriais, estes compostos acabam por surgir em águas de superfície. Apesar da sua relativamente reduzida toxicidade, estas substâncias químicas constituem uma ameaça para os ecossistemas aquáticos, uma vez que podem acumular em organismos aquáticos e adsorver a sedimentos e sólidos em suspensão. Os almíscares policíclicos são conhecidos por interferir com o sistema de resistência a multixenobióticos (MXR) das células e, em conjunto com o dietil ftalato (DEP), prejudicam a estrutura e funções celulares. Neste contexto, no presente estudo, foi avaliada a toxicidade dos almíscares policíclicos tonalide (AHTN) e galaxolide (HHCB) e o éster de ftalato DEP para a truta arco-íris (*Oncorhynchus mykiss*). Procedeu-se à exposição aguda *in vitro* de hepatócitos de *O. mykiss* a PCPs individuais e em misturas binárias. A citotoxicidade causada pelos PCPs foi avaliada através da aplicação das sondas fluorescentes alamar blue (AB), 5-carboxifluoresceína diacetato acetoximetil éster (CFDA-AM) e monoclorobimane (mBCI), que permitem medir o nível de atividade mitocondrial, integridade da membrana e estresse oxidativo da célula, respetivamente. Para além disso, foi avaliado o potencial dos PCPs individuais e em mistura de inibirem a atividade dos transportadores ABC nas células. De forma a compreender melhor a toxicidade de misturas, foram feitas comparações entre os resultados experimentais e as previsões dos modelos concentração adição (CA) e ação independente (IA). Os PCPs causaram efeitos citotóxicos em hepatócitos de *O. mykiss*, nomeadamente um decréscimo dose dependente na atividade mitocondrial e integridade da membrana celular e, indução de estresse oxidativo. Para os PCPs testados, os valores de EC<sub>50</sub> mais baixos corresponderam aos efeitos causados sob a integridade da membrana:  $111.40 \times 10^{-6}$  M para AHTN,  $3.67 \times 10^{-6}$  M para HHCB e  $25.31 \times 10^{-3}$  M para DEP. Relativamente ao estresse oxidativo, os hepatócitos parecem conseguir lidar com concentrações baixas de AHTN ( $0.02\text{--}23.3 \times 10^{-6}$  M), HHCB ( $0.02\text{--}2.3 \times 10^{-6}$  M) e DEP ( $2.3\text{--}20000 \times 10^{-6}$  M). No entanto, a concentrações mais elevadas, o sistema de defesa antioxidante parece ser prejudicado. Para além disso, os hepatócitos expostos a PCPs individuais e em mistura, apresentaram um decréscimo dose dependente na atividade dos transportadores ABC nas células. Assim, os compostos testados induziram efeitos citotóxicos em hepatócitos de truta arco-íris e inibiram o sistema de defesa MXR e, conseqüentemente, podem atuar como quimio-sensibilizantes. HHCB provou ser o composto mais tóxico para hepatócitos

de truta arco-íris, seguido do AHTN e DEP. As previsões dos modelos matemáticos indicaram interações toxicológicas entre as substâncias testadas, nomeadamente antagonismo no caso da mistura HHCB/DEP. Os efeitos da mistura AHTN/HHCB revelaram ser aditivos. De uma forma geral, estes resultados alertam para a importância de diagnosticar a presença de potenciais inibidores do sistema MXR no ambiente e, para a necessidade de investigar os efeitos tóxicos causados por misturas de substâncias químicas. Os organismos aquáticos, incluindo os peixes, tornam-se mais suscetíveis a potenciais efeitos adversos causados pela exposição a xenobióticos, se o sistema de defesa MXR estiver comprometido, especialmente na exposição a substâncias químicas que causam efeitos sinérgicos.



## Contents

<b>Abstract</b> .....	<b>i</b>
<b>Resumo</b> .....	<b>iii</b>
<b>List of Figures</b> .....	<b>vii</b>
<b>List of Tables</b> .....	<b>x</b>
<b>List of Abbreviations</b> .....	<b>xi</b>
<b>1. Introduction</b> .....	<b>1</b>
1.1. Personal care products .....	1
1.1.1. Synthetic musks .....	1
1.1.2. Phthalates .....	2
1.1.3. Fate and exposure .....	2
1.2. Toxicity testing .....	4
1.2.1. <i>In vivo</i> experimental models .....	5
1.2.2. <i>In vitro</i> models: cell cultures .....	5
1.2.3. Cytotoxicity testing .....	6
1.3. Cellular detoxification system .....	7
1.3.1. ABC transporters .....	8
1.3.2. Multixenobiotic resistance .....	9
1.4. Mixture toxicity .....	10
1.5. Aims and hypotheses .....	11
<b>2. Material and Methods</b> .....	<b>12</b>
2.1. Chemicals .....	12
2.2. Test organism .....	12
2.3. Primary cell culture .....	12
2.3.1. Hepatocytes isolation .....	12
2.3.2. Cell viability .....	13
2.3.3. Cell culture conditions .....	14
2.4. Exposure of hepatocytes to PCPs .....	14
2.4.1. General exposure conditions .....	14
2.4.2. Single exposure .....	14
2.4.3. Mixture exposure .....	15
2.5. Cytotoxicity testing .....	15

2.6. ABC transporter activity.....	16
2.7. Data analysis.....	17
<b>3. Results.....</b>	<b>19</b>
3.1. Cytotoxicity testing .....	19
3.1.1. Cell metabolic activity .....	19
3.1.2. Cell membrane integrity .....	20
3.1.3. Oxidative stress.....	22
3.2. ABC transporter activity.....	23
3.2.1. Experimental results .....	23
3.2.2. Model predictions .....	26
<b>4. Discussion .....</b>	<b>30</b>
4.1. Cytotoxicity testing .....	30
4.1.1. Cell metabolic activity and membrane integrity .....	30
4.1.2. Oxidative stress.....	31
4.2. ABC transporter activity.....	32
4.2.1. Experimental results .....	32
4.2.2. Model predictions .....	33
4.3. Assessment of primary hepatocyte viability .....	34
<b>5. Conclusions .....</b>	<b>36</b>
<b>References .....</b>	<b>38</b>
<b>Appendix I .....</b>	<b>44</b>
<b>Appendix II .....</b>	<b>48</b>

## List of Figures

**Figure 1.** Overview of oxidative stress induced by mechanisms such as redox cycling of xenobiotics (parent compound) and subsequent formation of reactive oxygen species (adapted from Di Giulio & Newman, 2013).

**Figure 2.** Models of the open and closed structure of ABC transporters (TMDs, transmembrane domains; NBDs, nucleotide-binding domains; adapted from: Cuthbertson *et al.*, 2010).

**Figure 3.** Mitochondrial activity of hepatocytes exposed to (A) AHTN, (B) HHCB, (C) DEP and (D) comparison of these three PCPs (% of control; mean  $\pm$  standard deviation; n = 2; dotted lines: 95% confidence interval; C: control).

**Figure 4.** Membrane integrity of hepatocytes exposed to (A) AHTN, (B) HHCB, (C) DEP and (D) comparison of these three PCPs (% of control; mean  $\pm$  standard deviation; n = 2; dotted lines: 95% confidence interval; C: control).

**Figure 5.** GSH content of hepatocytes exposed to (A) AHTN, (B) HHCB, (C) DEP and (D) comparison of these three PCPs (% of control; mean  $\pm$  standard deviation; n = 2; dotted lines: 95% confidence interval; C: control; red error bars: concentrations excluded from the non-linear regression curve fit).

**Figure 6.** Rho123 accumulation on hepatocytes exposed to the inhibitors (A) VER and (B) MK571 (% of control; mean  $\pm$  standard deviation; n = 2 for VER; n = 3 for MK571; dotted lines: 95% confidence interval; C: control; red error bars: concentrations excluded from the non-linear regression curve fit).

**Figure 7.** Rho123 accumulation on hepatocytes exposed to (A) AHTN, (B) HHCB, (C) DEP and (D) comparison of these three PCPs (% of MK571; mean  $\pm$  standard deviation; n = 3; dotted lines: 95% confidence interval; C: control; red error bars: concentrations excluded from the non-linear regression curve fit).

**Figure 8.** Rho123 accumulation on hepatocytes exposed to a mixture of (A) AHTN and HHCB (B) HHCB and DEP and (C) comparison of individual and mixed AHTN and HHCB and (D) individual and mixed HHCB and DEP (% of MK571; mean  $\pm$  standard deviation; n = 3; dotted lines: 95% confidence interval; C: control; red error bars: concentrations excluded from the non-linear regression curve fit).

**Figure 9.** CA model predictions of Rho123 accumulation on hepatocytes exposed to a mixture of (A) AHTN and HHCB (B) HHCB and DEP and (C) comparison of AHTN and HHCB experimental data with the model predictions and (D) HHCB and DEP experimental data with the model predictions (n = 3 for the experimental data; shade: 95% confidence interval).

**Figure 10.** IA model predictions of Rho123 accumulation on hepatocytes exposed to a mixture of (A) AHTN and HHCB (B) HHCB and DEP and (C) comparison of AHTN and HHCB experimental data with the model predictions and (D) HHCB and DEP experimental data with the model

predictions ( $n = 3$  for the experimental data; dotted lines and shade: 95% confidence interval; red dots: concentrations excluded from the non-linear regression curve fit).

**Figure 11.** Plate design for *O. mykiss* hepatocytes exposed to single compounds (AHTN, HHCB and DEP) and inhibitors (VER and MK571). Blank corresponds to wells only with cells, control corresponds to cells exposed to the solvent control DMSO and the remaining wells correspond to cells exposed to different concentrations of personal care products or inhibitors.

**Figure 12.** Plate design for *O. mykiss* hepatocytes exposed to a personal care products mixture of AHTN/HHCB and HHCB/DEP. Blank corresponds to wells only with cells and control corresponds to cells exposed to the solvent control DMSO. The remaining wells represent cells exposed to two PCPs with different concentrations (top line, concentration of 1st compound; bottom line, concentration of 2nd compound).

**Figure 13.** Mitochondrial activity of hepatocytes exposed to AHTN at the (A) first replicate (B) second replicate and (C) third replicate (% of control; mean  $\pm$  standard deviation; C: control).

**Figure 14.** Mitochondrial activity of hepatocytes exposed to HHCB at the (A) first replicate (B) second replicate and (C) third replicate (% of control; mean  $\pm$  standard deviation; dotted lines: 95% confidence interval; C: control).

**Figure 15.** Mitochondrial activity of hepatocytes exposed to DEP at the (A) first replicate (B) second replicate and (C) third replicate (% of control; mean  $\pm$  standard deviation; C: control).

**Figure 16.** Membrane integrity of hepatocytes exposed to AHTN at the (A) first replicate (B) second replicate and (C) third replicate (% of control; mean  $\pm$  standard deviation; dotted lines: 95% confidence interval; C: control).

**Figure 17.** Membrane integrity of hepatocytes exposed to HHCB at the (A) first replicate (B) second replicate and (C) third replicate (% of control; mean  $\pm$  standard deviation; dotted lines: 95% confidence interval; C: control).

**Figure 18.** Membrane integrity of hepatocytes exposed to DEP at the (A) first replicate (B) second replicate and (C) third replicate (% of control; mean  $\pm$  standard deviation; C: control).

**Figure 19.** GSH content of hepatocytes exposed to AHTN at the (A) first replicate (B) second replicate and (C) third replicate (% of control; mean  $\pm$  standard deviation; C: control; red error bars: concentrations excluded from the graphical analysis).

**Figure 20.** GSH content of hepatocytes exposed to HHCB at the (A) first replicate (B) second replicate and (C) third replicate (% of control; mean  $\pm$  standard deviation; C: control; red error bars: concentrations excluded from the non-linear regression curve fit and graphical analysis).

**Figure 21.** GSH content of hepatocytes exposed to DEP at the (A) first replicate (B) second replicate and (C) third replicate (% of control; mean  $\pm$  standard deviation; C: control; red error bars: concentrations excluded from the graphical analysis).

**Figure 22.** Rho123 accumulation on hepatocytes exposed to the inhibitor VER at the (A) first replicate (B) second replicate and (C) third replicate (% of control; mean  $\pm$  standard deviation; dotted lines: 95% confidence interval; C: control; red error bars: concentrations excluded from the non-linear regression curve fit).

**Figure 23.** Rho123 accumulation on hepatocytes exposed to the inhibitor MK571 at the (A) first replicate (B) second replicate and (C) third replicate (% of control; mean  $\pm$  standard deviation; dotted lines: 95% confidence interval; C: control; red error bars: concentrations excluded from the non-linear regression curve fit).

**Figure 24.** Rho123 accumulation on hepatocytes exposed to AHTN at the (A) first replicate (B) second replicate and (C) third replicate (% of MK571; mean  $\pm$  standard deviation; dotted lines: 95% confidence interval; C: control; red error bars: concentrations excluded from the non-linear regression curve fit).

**Figure 25.** Rho123 accumulation on hepatocytes exposed to HHCB at the (A) first replicate (B) second replicate and (C) third replicate (% of MK571; mean  $\pm$  standard deviation; dotted lines: 95% confidence interval; C: control; red error bars: concentrations excluded from the non-linear regression curve fit).

**Figure 26.** Rho123 accumulation on hepatocytes exposed to DEP at the (A) first replicate (B) second replicate and (C) third replicate (% of MK571; mean  $\pm$  standard deviation; dotted lines: 95% confidence interval; C: control; red error bars: concentrations excluded from the non-linear regression curve fit).

**Figure 27.** Rho123 accumulation on hepatocytes exposed to a mixture of AHTN and HHCB at the (A) first replicate (B) second replicate and (C) third replicate (% of MK571; mean  $\pm$  standard deviation; dotted lines: 95% confidence interval; C: control; red error bars: concentrations excluded from the non-linear regression curve fit).

**Figure 28.** Rho123 accumulation on hepatocytes exposed to a mixture of HHCB and DEP at the (A) first replicate (B) second replicate and (C) third replicate (% of MK571; mean  $\pm$  standard deviation; dotted lines: 95% confidence interval; C: control; red error bars: concentrations excluded from the non-linear regression curve fit).

## List of Tables

**Table 1.** Identification and physico-chemical properties of three widely used personal care products (AHTN: tonalide; HHCB: galaxolide; DEP: diethyl phthalate; from PubChem, 2014).

**Table 2.** Parameters (body weight and body length) of *Oncorhynchus mykiss* replicates and respective number of isolated and viable cells after hepatocyte isolation.

**Table 3.** Personal care products  $EC_{50}$  values and respective 95% confidence interval for mitochondrial activity of hepatocytes, derived from a non-linear regression curve fit.

**Table 4.** Personal care products  $EC_{50}$  values and respective 95% confidence interval for membrane integrity of hepatocytes, derived from a non-linear regression curve fit.

**Table 5.** Personal care products  $EC_{50}$  values and respective 95% confidence interval for GSH content of hepatocytes, derived from a non-linear regression curve fit.

**Table 6.** Inhibitors  $EC_{50}$  values and respective 95% confidence interval for rhodamine 123 accumulation on hepatocytes, derived from a non-linear regression curve fit.

**Table 7.** Personal care products  $EC_{50}$  values and respective 95% confidence intervals for rhodamine 123 accumulation on hepatocytes, derived from a non-linear regression curve fit.

**Table 8.** Experimental and predicted  $EC_{50}$  values and respective 95% confidence interval for rhodamine 123 accumulation on hepatocytes exposed to a mixture of AHTN and HHCB, derived from a non-linear regression curve fit (CA: concentration addition; IA: independent action).

**Table 9.** Experimental and predicted  $EC_{50}$  values and respective 95% confidence interval for rhodamine 123 accumulation on hepatocytes exposed to a mixture of HHCB and DEP, derived from a non-linear regression curve fit (CA: concentration addition; IA: independent action).

**Table 10.** Chemicals used throughout the experiment.

**Table 11.** Composition of solutions used throughout the experiment. These solutions were sterilized by filtration (0.22  $\mu\text{m}$ ).

## List of Abbreviations

$\cdot\text{O}_2^-$	Superoxide anion radical
AB	Alamar blue
ABC	ATP-binding cassette
AHTN	6-acetyl-1,1,2,4,4,7-hexamethyltetralin
ATP	Adenosine triphosphate
BSA	Bovine serum albumin
CA	Concentration addition
CF	5-carboxyfluorescein
CFDA-AM	5-carboxyfluorescein diacetate acetoxymethyl ester
CI	Confidence interval
CO <sub>2</sub>	Carbon dioxide
DEP	Diethyl phthalate
DMSO	Dimethyl sulfoxide
EC <sub>50</sub>	50% effective concentration – the concentration that induces 50% of effect on the tested population in the specific conditions of the test
EGTA	Ethylene glycol tetraacetic acid
GPx	Glutathione peroxidase
GR	Glutathione reductase
GSH	Glutathione
GSSG	Glutathione disulfide
GST	Glutathione S-transferases
H <sub>2</sub> O <sub>2</sub>	Hydrogen peroxide
HHCB	1,3,4,6,7,8-hexahydro-4,6,6,7,8,8-hexamethylcyclopenta-[g]-2-benzopyran
IA	Independent action
IUPAC	International union of pure and applied chemistry
mBCl	Monochlorobimane
MMP	Mitochondrial membrane permeabilization
MRP	Multidrug resistance-associated protein
MXR	Multixenobiotic resistance
NBD	Nucleotide-binding domain
PBS	Phosphate buffered saline
PCPs	Personal care products
P-gp	P-glycoprotein

PPCPs	Pharmaceuticals and personal care products
Rho123	Rhodamine 123
ROS	Reactive oxygen species
RTG-2	Rainbow trout gonad cell line
RTL-W1	Rainbow trout liver cell line
SD	Standard deviation
TMD	Transmembrane domain
UV	Ultraviolet
VER	Verapamil hydrochloride



## 1. Introduction

### 1.1. Personal care products

Personal care products (PCPs) are a group of compounds used in a wide range of products including fragrances, disinfectants, insect repellants, preservatives and UV filters (Brausch & Rand, 2011). Large amounts of these chemicals are produced and consumed worldwide and consequently released into the environment. As foreign substances to the organism - xenobiotics - these chemicals constitute a class of priority pollutants known as pharmaceuticals and personal care products (PPCPs). So far, the main focus in this field has been the study of the adverse effects of pharmaceuticals on non-target organisms and on ecosystems; PCPs have not received sufficient attention due to their assumed relatively low toxicity and environmental risk. However, it has to be taken into consideration the presence of PCPs in the aquatic ecosystem and their potential to affect non-target organisms through interference with multixenobiotic resistance (MXR) efflux transporters (Luckenbach & Epel, 2005). Even if certain chemicals themselves have a non-toxic to slightly toxic effect on aquatic organisms, they might be responsible for inhibiting the MXR defense system of cells, leading to an intracellular accumulation of xenobiotics and a more susceptible individual (Smital *et al.*, 2004). Brausch & Rand (2011) discovered that in aquatic environments, PCPs have been found more frequently and at higher concentrations than pharmaceuticals. As a result of their continuous release into sewers, these chemicals are commonly detected in surface waters and become persistent in the environment. Furthermore, some PCPs are bioactive and have the potential to bioaccumulate in aquatic organisms (Brausch & Rand, 2011).

#### 1.1.1. Synthetic musks

The use of natural musk fragrances was overtaken for decades. Since the 1950s, synthetic musks became an easy and cheap solution to fill the world with scent but around the 1980s they started to be detected in the environment and be seen as a potential health threat (Bester, 2009). A huge variety of products contain these artificial fragrances, including perfumes, creams, soaps, detergents and deodorants (Nakata *et al.*, 2007). Synthetic musks can be divided into three major classes: nitro-aromatic, polycyclic and macrocyclic musks (Bester, 2009). Nowadays, polycyclic musks are prevalent in the market since they are widely used in replacement of certain nitro musks whose usage was banned or reduced (Hutter *et al.*, 2009; International Fragrance Association, 2011). In 1987, polycyclic musks comprised 61% of the total amount of synthetic musks produced in the world. The trend seems to be an increasing production and usage of polycyclic

musks over the years, particularly Tonalide<sup>®</sup> (AHTN) and Galaxolide<sup>®</sup> (HHCB), which are produced in very high volumes in both Europe and the United States (Nakata *et al.*, 2007). The main fragranced products containing polycyclic musks are cosmetics and household cleaning products, which in the future will possibly be replaced by macrocyclic musks for having a more intensive smell and requiring lower concentrations (Bester, 2009).

### 1.1.2. Phthalates

Phthalate esters are a family of chemicals mainly used as plasticizers and softeners to produce more flexible and resilient polymers. In addition to its application in numerous consumer products made of plastic and vinyl (toys, food packaging, electronics, medical devices, building materials), phthalates are frequently used in cosmetics and personal care products to make fragrance or color last longer, since they have a fixation capacity (Zheng *et al.*, 2013; Hubinger, 2010). They are included in perfumes, bath products, lotions, hair sprays, nail polish and detergents (Kang *et al.*, 2010). In cosmetics, they can perform the function of skin moisturizers, skin softeners and skin penetration enhancers (Hubinger, 2010). Phthalates are not covalently bound to raw materials and therefore can be easily released into the environment through leaching, migration and evaporation processes (Zheng *et al.*, 2013). This results in the presence of these chemicals in water ecosystems at measurable concentrations due to its increasing production and constant release in effluents (Zheng *et al.*, 2013). The most common phthalate used as solvent and vehicle for fragrance and cosmetic ingredients is diethyl phthalate (DEP; American Chemistry Council, 2014). Its main environmental contamination sources are the synthesis processes and the utilization and disposal of its final products with consequent leaching from landfill sites (Kang *et al.*, 2010). Although DEP is present in all environmental compartments, water contamination generates the greatest concern (Hubinger, 2010).

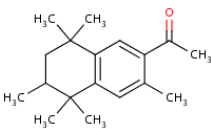
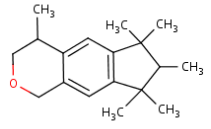
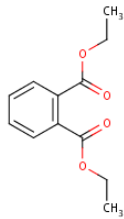
### 1.1.3. Fate and exposure

The aquatic ecosystems may be the final reservoir for xenobiotics intentionally or accidentally released into the environment. As mentioned earlier, the environment is constantly being subjected to the presence of anthropogenic contaminants that endanger the natural functions of an ecosystem. Personal care products are not an exception. Continuously discharged in effluents, they end up in freshwater and marine environments and eventually accumulate in sediments, sludges and biota due to their lipophilic nature (Bester, 2009). This lends to PCPs some characteristics of persistent pollutants, despite their degradability and relative short environmental half-lives. This means, organisms that

are in constant contact with contaminated water, especially those living close to wastewater treatment facilities, concentrate the substances from the water but, at the same time, are able to transform them to more polar metabolites that are more easily excreted; half-lives of chemicals in water are therefore considerably reduced (Balk & Ford, 1999). However, the octanol-water coefficients of the selected PCPs suggest a high potential for bioaccumulation in aquatic organisms, especially for polycyclic musks (PubChem, 2014); overview of physico-chemical properties in **Table 1**. This kind of behavior makes it difficult to predict the residence time of PCPs in aquatic ecosystems. Based on their vapor pressure, water solubility and consequently the estimated Henry's Law constant, polycyclic musks are expected to volatilize from surface waters (PubChem, 2014). However, polycyclic musks are also expected to precipitate to the bottom of the sea and adsorb to suspended solids and sediments, which in turn attenuates volatilization from water and increases chemicals half-lives (PubChem, 2014). Diethyl phthalate is not expected to volatilize from surface waters but adsorption to suspended solids and sediments seems to be an important fate process (PubChem, 2014). Contrary to the polycyclic musks, DEP is expected to hydrolyze (slowly) in the environment and biodegradation in the aquatic environment seems to play a major role (PubChem, 2014). Previous findings indicate that polycyclic musks accumulate in mussels, crustaceans, fish and even in organisms at higher trophic levels, including coastal birds and mammals in marine ecosystems (Nakata *et al.*, 2007; Ramirez *et al.*, 2009). Taking this into consideration, bioaccumulation can occur through direct contact with the water and the contaminated seabed and/or through food chain transfer. The latter one makes benthic organisms more susceptible to exposure to PCPs (Nakata *et al.*, 2007). Another important factor that influences the presence of PCPs in organisms is their lipid content. Compounds which do not possess ionizable functional groups, such as polycyclic musks, have a positive correlation with tissue lipid content (Ramirez *et al.*, 2009). As known, hydrophobic compounds concentrate more easily in tissues with high lipid content, such as the liver. This was confirmed by a national pilot study conducted by Ramirez *et al.* (2009) in the United States, where different fish species were screened for the presence of PPCPs in their tissues and the results showed that higher concentration and frequencies of compounds are detected in livers in comparison with fillets. AHTN and HHCB were detected in fish from all the five rivers, with maximum concentrations ranging from 21–290 ng/g and 300–2100 ng/g, respectively (Ramirez *et al.*, 2009). In trout from Danish fish farms, lower concentrations of polycyclic musks were detected: 2.24–2.70 ng/g fresh weight for AHTN and 5.87–8.54 ng/g fresh weight for HHCB (Duedahl-Olesen *et al.*, 2005). According to Brausch & Rand (2011), polycyclic musks are found in European rivers at concentrations ranging between 2–300 ng/L, with HHCB being

detected at the higher levels. Regarding the environmental concentrations of DEP, a study conducted in India revealed that this phthalate is present along the river Kaveri with a mean level of 241 ng/L (Selvaraj *et al.*, 2014). This value is similar to the concentrations detected in European rivers of Spain and Sweden which range between 10–280 ng/L. However, in surface waters from the Netherlands, DEP was detected at much higher levels, reaching values of 2300 ng/L (Vethaak *et al.*, 2005). In sediments from these rivers was verified the same tendency; in India DEP was present at a mean level of 16.5 ng/g and in the Netherlands at concentrations ranging between 65–1200 ng/g dry weight (Selvaraj *et al.*, 2014; Vethaak *et al.*, 2005). In muscle tissue of estuarine and freshwater fish, DEP was detected at concentration ranges of 6.7–91 ng/g wet weight in flounder and 22–321 ng/g wet weight in bream (Vethaak *et al.*, 2005).

**Table 1.** Identification and physico-chemical properties of three widely used personal care products (AHTN: tonalide; HHCB: galaxolide; DEP: diethyl phthalate; from PubChem, 2014).

	AHTN	HHCB	DEP
<b>Molecular formula</b>	C <sub>18</sub> H <sub>26</sub> O	C <sub>18</sub> H <sub>26</sub> O	C <sub>12</sub> H <sub>14</sub> O <sub>4</sub>
<b>IUPAC name</b>	1-(3,5,5,6,8,8-hexamethyl-6,7-dihydronaphthalen-2-yl)ethanone	4,6,6,7,8,8-hexamethyl-1,3,4,7-tetrahydrocyclopenta[ <i>g</i> ]isochromene	Diethyl benzene-1,2-dicarboxylate
<b>Structural formula</b>			
<b>Molecular weight (g/mol)</b>	258.4	258.4	222.24
<b>Physical state</b>	solid	viscous liquid	oily liquid
<b>Solubility in water (mg/L)</b>	1.25	1.75	1080
<b>Octanol/Water Partition Coefficient (log K<sub>ow</sub>)</b>	5.7	5.9	2.47
<b>Vapor pressure (mm Hg)</b>	5.12 × 10 <sup>-4</sup>	5.45 × 10 <sup>-4</sup>	2.1 × 10 <sup>-3</sup>
<b>Henry's law constant (atm-cu m/mol)</b>	1.393 × 10 <sup>-4</sup>	1.32 × 10 <sup>-4</sup>	6.10 × 10 <sup>-7</sup>

## 1.2. Toxicity testing

In toxicological testing, the potential adverse effects of chemicals on living systems and the mechanisms of toxicity involved are assessed. For this purpose, intact animals or cell cultures can be used in a diversity of *in vivo* and *in vitro* tests. To establish a dose-

response relationship, selected concentration ranges of chemicals are used (Robinson & Thorn, 2005). Typically, toxicity tests use whole animals that are exposed to high doses of the chemical to be tested. However, alternatives to these methods have been developed to enable faster screening of chemicals and reduce and/or replace the use of laboratory animals. An increasing number of cells, cellular components and tissues have been used to evaluate the effects of chemicals on a molecular level. The use of *in vitro* model systems allows a better understanding of the cellular response pathways that may lead to adverse health effects on living organisms (National Research Council, 2007). Furthermore, this system reduces the quantity of chemicals needed for testing and the costs associated with the maintenance of animals (Soldatow *et al.*, 2013).

#### 1.2.1. *In vivo* experimental models

Experimental model organisms are non-human species used for research purposes to investigate a specific biological process or system. These experimental organisms can be used to understand a number of phenomena that occur in the environment through more simplified *in vivo* models. It is important to take into account that data obtained from less developed organisms can be a useful tool to predict behavior of chemicals in similar species or more distant and complex organisms. In general, experimental model organisms are easy to breed and maintain on a large scale under laboratory conditions and can be considered mediators between theory and reality (Ankeny & Leonelli, 2011). An experimental model can be chosen according to their biochemical and physiological functions and ecological relevance. Fish are relevant species for environmental monitoring studies due to their role in the aquatic trophic chain and similarity to higher vertebrates, in terms of responses to toxic substances. Fish represents an extremely diverse and large group of vertebrates that have the ability to adapt to a wide range of environments (Harris *et al.*, 2014). As good models for environmental biology studies they might serve as first insight into the presence of xenobiotics in the environment. One of the most common representatives of coldwater species used in fish research is rainbow trout, *Oncorhynchus mykiss* (Ostrander, 2000).

#### 1.2.2. *In vitro* models: cell cultures

Although *in vivo* models resemble more what happens in a natural environment and the complex biological processes and interactions that occur during exposure of organisms to xenobiotics, *in vitro* models have been increasingly used in toxicological studies (Ostrander, 2000). It is important to evaluate the potential effects of chemicals starting from a cellular and molecular level, which is possible through the use of *in vitro* models. In

this way, chemicals can be screened more quickly and easily for its mechanism of action. This can be done by using fish cell cultures prepared from different tissues and organs. The term cell culture can be applied to two different types of cultures: primary cultures and cell lines. Primary cultures are cells obtained directly from the fish and maintained under *in vitro* conditions whereas cell lines are cultures obtained from the subculturing or passaging of primary cultures (Ostrander, 2000). Primary cultures mimic more closely the function and physiological state of cells *in vivo* than cell lines and are widely used models in the field of (eco)toxicology (Ostrander, 2000). Good examples are the primary fish hepatocyte cultures, important to assess metabolic activity and mechanisms of toxicity *in vitro* (Schreer et al., 2005). The liver is an organ of extreme importance in vertebrates for being crucial in the maintenance of internal homeostasis and being the major site of metabolism; therefore widely used in toxicity testing (Segner, 1998). Primary hepatocyte cultures are useful tools for enzyme induction and inhibition studies since they are able to maintain functional activities for 24–72 hours (Soldatow et al., 2013). However, some cell culture conditions should be fulfilled to maintain viable cells for an extended period of time and preserve the functional properties of cells. In primary cultures of fish cells, attention should be given to adjustments in parameters such as temperature, osmolality, pH and CO<sub>2</sub> partial pressure (Hodne et al., 2012).

### 1.2.3. Cytotoxicity testing

To evaluate the effects of chemicals on the viability of cells is a widely used method. Therefore, the number of metabolically active cells in culture is measured; cells are exposed to a metabolic indicator that interacts with cellular enzymes and consequently is converted into a measurable fluorescent or luminescent compound (Stoddart, 2011). For instance, once the non-fluorescent dye resazurin enters in contact with viable cells it is reduced into the fluorescent compound resorufin (Stoddart, 2011). Through the use of cytotoxicity assays it is possible to better understand the mode of action of chemicals. For instance, when cells become unviable, gene expression can be affected (Schreer et al., 2005). Polycyclic musks are potential inducers of cytotoxic effects on rainbow trout cells. Schnell et al. (2009) monitored cell viability on RTL-W1 liver cells exposed to polycyclic musks by using two fluorescent dyes (AB and CFDA-AM) and concluded that these are cytotoxic to a fish liver cell line, specially tonalide. This is consistent with findings from Randelli et al. (2011), which suggest that tonalide could be a potential inducer of early apoptosis and is capable of affecting gene expression in rainbow trout. However, information about the toxicological mechanisms of action of PCPs on fish primary cell cultures is limited.

### 1.3. Cellular detoxification system

Metabolism of xenobiotics occurs through successive reaction within cells. This biotransformation process aims to decrease toxicity of xenobiotics and generate compounds that are easier to eliminate. However, the toxicity of certain compounds can be increased when more reactive metabolites are generated. Phase I and phase II enzymes, that predominate in the liver, are responsible for the metabolism of xenobiotics. Phase I enzymes have the ability to transform lipophilic xenobiotics in more polar metabolites and provide sites for conjugation reactions (Hodgson, 2010). Phase II enzymes are involved in the conjugation of these xenobiotic metabolites with endogenous metabolites, including glutathione (GSH), sugars and amino acids (Hodgson, 2010). One example of phase II enzyme is glutathione S-transferase (GST), which conjugates GSH with compounds containing electrophilic centers (Croom, 2012). GSH is important in the cellular defense against agents that cause oxidative stress because it removes reactive electrophiles and therefore protects cells from the action of radicals via the glutathione redox cycle; general oxidative stress process in **Figure 1**. Oxidative stress results from the imbalance between production of reactive oxygen species (ROS) and its decomposition through antioxidant defense mechanisms (Chen *et al.*, 2012). In the presence of an excessive amount of ROS, e.g. superoxide anion ( $\text{O}_2^-$ ) and hydrogen peroxide ( $\text{H}_2\text{O}_2$ ), cells enter oxidative stress processes (Di Giulio & Newman, 2013). The GSH-dependent antioxidant defense mechanism is of great importance in the cell defenses against adverse effects of ROS; enzymes such as glutathione peroxidase (GPx) and glutathione reductase (GR) play a major role (Zhang, 2014). Interaction of xenobiotics with the electron transport chain may generate  $\text{O}_2^-$  and consequently  $\text{H}_2\text{O}_2$ , which are cleared through the action of enzymes such as glutathione peroxidase (Di Giulio & Newman, 2013; Zhang, 2014). In the absence of stress, cells contain a high intracellular ratio of reduced glutathione (GSH) to oxidized glutathione (GSSG; Hodgson, 2010). Once metabolism of xenobiotics is over, compounds resulting from this process need to be eliminated. This is possible through passive transport (diffusion of molecules across cellular membranes) or active transport with the intervention of transporter proteins. These proteins require energy to transport the compounds against the concentration gradient (Croom, 2012).

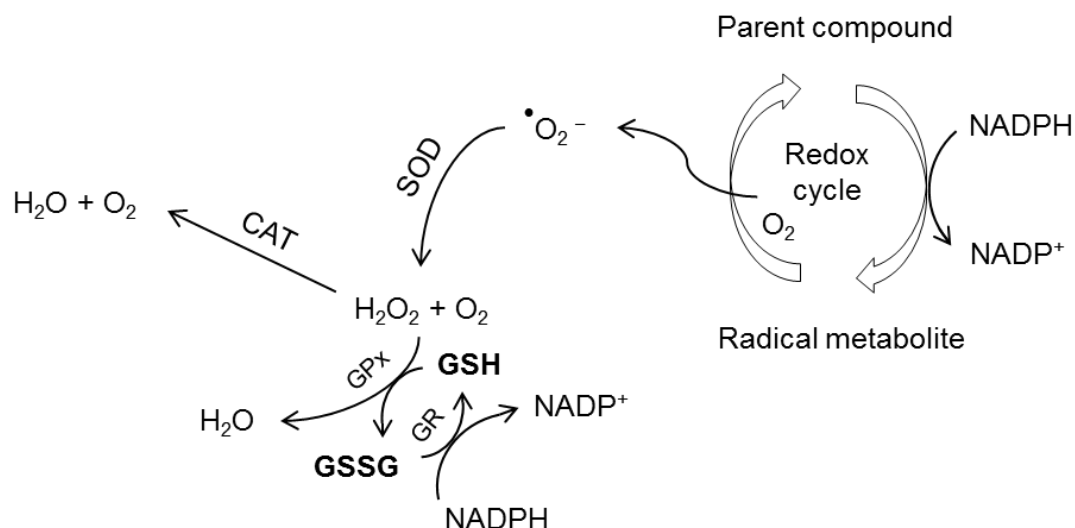


**Figure 1.** Overview of oxidative stress induced by mechanisms such as redox cycling of xenobiotics (parent compound) and subsequent formation of reactive oxygen species (adapted from Di Giulio & Newman, 2013).

### 1.3.1. ABC transporters

ATP-binding cassette (ABC) transporters are a large family of proteins that have been conserved across the animal kingdoms and can be found in all species from bacteria to man (Higgins, 2001). These proteins are an integral part of the cellular detoxification system and are mostly involved in the translocation of endogenous and exogenous substances across the membrane, including the excretion of chemicals from the cell through efflux pumps (Choi, 2005). ABC transporters use the hydrolysis of ATP to pump non-polar compounds from the membrane bilayer out of the cell, including xenobiotics (Choi, 2005). These transporters are composed of four main domains: two transmembrane domains (TMDs) and two hydrophilic nucleotide-binding domains (NBDs; also known as ABC domains) that face the cytoplasm; schematic representation in **Figure 2**. The domains can be encoded as single polypeptides or be fused in any possible combination (Higgins, 2001). Mammalian and fish ABC genes are organized in subfamilies categorized from ABCA to ABCH; the latter one is exclusively for fish (Lončar *et al.*, 2010). Despite the existence of numerous ABC proteins, P-glycoproteins (Pgp; ABCB1) and multidrug resistance-associated proteins 1–5 (MRP1–5; ABCC1–5) revealed to be among the toxicologically most relevant proteins in mammalian tissues; they possess MXR-related functions (Lončar *et al.*, 2010; Faria *et al.*, 2011). ABC proteins are present in aquatic organisms inclusive in mussels, sea urchin, sea star and rainbow trout tissues (liver, kidney, intestine, gonads, brain; Lončar *et al.*, 2010; Faria *et al.*, 2011).



Several subfamilies of transporters are expressed in these tissues: in liver, high expression of ABCB1, ABCB11 and ABCC2 were detected (Lončar *et al.*, 2010). According to Zaja *et al.* (2008), primary trout hepatocytes also express components of the detoxification system, including phase I and II enzymes and ABC proteins.

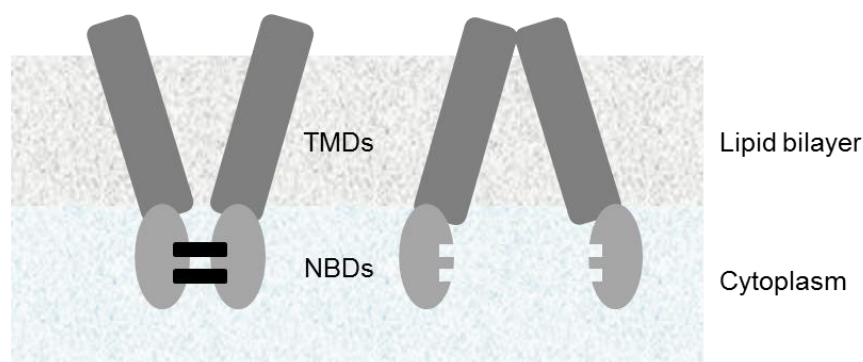


**Figure 2.** Models of the open and closed structure of ABC transporters (TMDs, transmembrane domains; NBDs, nucleotide-binding domains; adapted from: Cuthbertson *et al.*, 2010).

### 1.3.2. Multixenobiotic resistance

In aquatic organisms, the defense mechanism associated with the functioning of the ABC transporters against xenobiotics is known as multixenobiotic resistance (MXR; Zaja *et al.*, 2008). Although ABC transporters are specific for its substrate(s), it should be noted that these proteins transport a wide spectrum of substances and that xenobiotics entering the cell can bind to the ABC proteins and consequently inhibit their function (Higgins, 2001). Thus, xenobiotics normally effluxed by ABC transporters are retained and accumulated in the cells leading to higher toxicity levels (Smital *et al.*, 2004). Innumerable inhibitors of the MXR defense system are present in the environment, making organisms more susceptible to exposure to potentially toxic substances. For this reason, MXR inhibitors are considered chemosensitizers; they will increase chemosensitivity of organisms towards xenobiotics present in their environment (Smital *et al.*, 2004). Chemosensitizers can be divided into two groups based on their mechanism of action: competitive inhibitors and non-competitive inhibitors (Faria *et al.*, 2011). The first act as substrates with high affinity for ABC protein binding sites, saturating the substrate-binding capacity of transporters, thus preventing the binding and transport of other substances (Smital *et al.*, 2004; Faria *et al.*, 2011). Examples of competitive inhibitors are verapamil and MK571 (Smital *et al.*, 2004; Keppler, 2011). Non-competitive inhibitors can act in different ways e.g., they can block the ATPase activity of transporters necessary for its proper functioning (Smital *et al.*, 2004). Examples of xenobiotics that have a MXR inhibitory potential in aquatic organisms

are the polycyclic musks (Smital *et al.*, 2004). Luckenbach & Epel (2005) showed that these compounds inhibit the activity of ABC efflux transporters in gills of the marine mussel *Mytilus californianus*. Despite the progresses in this field, knowledge about the interference of chemicals with ABC transporters in fish remains scarce; it is therefore of major importance to consider indirect effects of PCPs on aquatic organisms.

#### **1.4. Mixture toxicity**

In risk assessment, chemicals are mostly evaluated as single substances. In the first instance, assessing the effect of single compounds can be sufficient to establish thresholds below which each chemical can be allowed to be used. However, environmental contamination is a consequence of the release of innumerable chemicals from various sources, resulting in complex mixtures of chemicals that need to be assessed (Cedergreen *et al.*, 2008). Mixtures of chemicals sometimes induce greater biological effects on organisms and in concentration ranges where single chemicals do not show effects (Thorpe *et al.*, 2006; Baas *et al.*, 2010). Considering this, it is important to predict combined effects of chemical mixtures, which is sometimes possible through exploitation of single-substance toxicity data (Cedergreen *et al.*, 2008). Mathematical modeling has been seen as a suitable tool to relate chemicals present in the environment at a given concentration to a predicted biological effect (Thorpe *et al.*, 2006). In binary mixtures, if the effects of single compounds and respective concentrations in the mixture are known, the most frequently used models to predict joint effects in ecotoxicology are the concentration addition (CA; also known as Loewe additivity) model and the independent action (IA; also known as Bliss independence) model (Backhaus & Faust, 2012; Cedergreen *et al.*, 2008). CA assumes that chemicals have a similar mechanism of action, which means, for example, that they bind to the same receptor and therefore can be considered as dilutions of one another (Backhaus & Faust, 2012; Cedergreen *et al.*, 2007). In turn, IA assumes that chemicals have a dissimilar mechanism of action. Experimental results can easily be compared to these reference models, in order to evaluate the joint effects of chemicals. If the effect of a mixture and respective CA model predictions are similar, chemicals are said to be additive (Cedergreen *et al.*, 2007). However, when the effect of a mixture differs significantly from the model predictions, it means that interactions occur, which either can be synergistic or antagonistic (Baas *et al.*, 2010; Cedergreen *et al.*, 2007). If the joint effect of two chemicals gives a higher effect than the model prediction, the effect is said to be synergistic. If the opposite occurs, the effect of the chemicals is said to be antagonistic (Cedergreen *et al.*, 2007). CA is

considered the best and more conservative reference model for chemical mixtures with similar target sites (Cedergreen *et al.*, 2008).

### **1.5. Aims and hypotheses**

The central objective of the present study was to *evaluate the toxicity of three PCPs (AHTN, HHCB and DEP), alone and in binary mixtures, to O. mykiss hepatocytes*. The following hypotheses were tested:

- 1) Exposure to PCPs causes a dose-dependent cytotoxic effect on *O. mykiss* hepatocytes;
- 2) There is a dose-dependent decrease in ABC transporter activity of *O. mykiss* hepatocytes after exposure to single PCPs;
- 3) Toxicological interactions with effects on hepatocytes ABC transporter activity occur under hepatocyte exposure to binary mixtures of the tested PCPs.

## 2. Material and Methods

### 2.1. Chemicals

Polycyclic musks 6-acetyl-1,1,2,4,4,7-hexamethyltetralin (AHTN) and 1,3,4,6,7,8-hexahydro-4,6,6,7,8,8-hexamethylcyclopenta-[g]-2-benzopyran (HHCB) solution, as well as diethyl phthalate, monochlorobimane (mBCI) and verapamil hydrochloride were purchased from Sigma-Aldrich (Schnelldorf, Germany). Alamar blue (AB) and 5-carboxyfluorescein diacetate acetoxymethyl ester (CFDA-AM) were obtained from Invitrogen Life Technologies (Paisley, Scotland). MK571 and rhodamine 123 were obtained from Cayman Chemical (Ann Arbor, Michigan, USA) and Molecular Probes (Paisley, Scotland), respectively. The chemicals used throughout the experiment are listed in detail in **Table 10**, Appendix I.

### 2.2. Test organism

Juvenile *Oncorhynchus mykiss* (body length, 20–30 cm) were obtained from a local fish farm (Ås, Akershus) and kept in tanks at the Department of Biology, University of Oslo. Water conditions were maintained at 7–8 °C, pH 7, with approximately 100% oxygen saturation. The light was adjusted to a day/night cycle of 12/12 h. Rainbow trout were fed once a day with Spirit Ørret 300 (4.5 mm) fish pellets (Skretting Averøy, Averøy, Norway).

### 2.3. Primary cell culture

#### 2.3.1. Hepatocytes isolation

*O. mykiss* hepatocytes were isolated according to the perfusion technique described by Ellesat *et al.* (2010). This procedure required a perfusion buffer (**Table 11**, Appendix I) that was previously prepared and kept at 4 °C. Fish were sacrificed with a blow to the head and the body surface was disinfected by using 70% ethanol. The body cavity was carefully opened from the urogenital pore to the pectoral fin to access the portal vein, liver and heart, without damaging the organs. A cannula was inserted into the portal vein that leads to the liver and perfusion buffer, containing EGTA (26 µM), was used to initially perfuse the liver. After a few seconds, the liver obtained a lighter colour and the heart was opened to allow the outflow of blood. This perfusion buffer was used during 10–15 min, until the liver has reached a yellow appearance and was without blood. Sometimes it was necessary to gently massage the liver to allow better clearance from blood or to remove blood clots that were impeding the outflow of blood from the heart. For the digestion, the liver was perfused (10–15 min) with the perfusion buffer containing 0.3 mg/mL

collagenase VIII and CaCl<sub>2</sub> (2 mM). After removing the cannula, the digested liver was transferred into a glass tray and gently mixed (10 min) in ice-cold perfusion buffer containing 0.1% (w/v) BSA, to separate the cells. The cell suspension was filtered through sterile 200 µm and 100 µm nylon meshes (Bigman AB, Sundbyberg, Sweden). Filtered liver cells were centrifuged three times at 500 rpm (27× g) for 3–4 min at 4 °C, using an Eppendorf 5810R Centrifuge (Eppendorf, Hamburg, Germany). The supernatant was discarded and the hepatocytes were re-suspended in perfusion buffer containing BSA. After the last centrifugation, the hepatocytes were re-suspended in sterile filtered (0.22 µm) Leibovitz's L-15 medium (pH 7.6, 310 mOsm) with 0.3 mg/mL L-glutamine. Sodium bicarbonate solution (4.5 mM) and an antibiotic antimycotic mix (100×) were added to reach a final concentration of penicillin, streptomycin and amphotericin B of 100 U/mL, 100 µg/mL and 0.25 µg/mL, respectively. The cells were filtered once more through a sterile 100 µm nylon mesh and kept on ice. To improve the quality of the cultures and reduce certain stress factors, osmolality of the medium and working solutions were adjusted to the plasma osmolality of rainbow trout (310 mOsm) with Knauer Osmometer Automatic (Knauer, Berlin, Germany; Al-Jandal & Wilson, 2011; Hodne *et al.*, 2012). All glassware and instruments were autoclaved before use.

### 2.3.2. Cell viability

To determine the number of viable cells, the trypan blue exclusion assay was used (Stoddart, 2011). This assay is based on the dye exclusion capability of living cells, since they possess intact cell membranes. Thus, viable cells are easy to detect due to their clear cytoplasm and dead cells are detectable by their blue stained cytoplasm, since these cells take up the dye. Cells were diluted 1:3 in trypan blue and counted in a Bürker-Türk counting chamber. Exposure of cells to trypan blue should not exceed 15 min because also viable cells may start to take up the dye (Frei, 2011). An area of 0.064 mm<sup>2</sup> was counted four times and the average value of viable cells was used in the following formula, in order to obtain number of cells/mL:

$$cells/mL = \frac{number\ of\ cells}{counted\ area\ (mm^2) \times chamber\ depth\ (mm) \times dilution} \times 1000$$

Cells were only used for experiments if the viability was larger than 85%. The amount of collected cells was sufficient to meet the required volume (~200 mL) for each experimental replicate; measured parameters of each fish replicate and respective cell viability in **Table 2**.

**Table 2.** Parameters (body weight and body length) of *Oncorhynchus mykiss* replicates and respective number of isolated and viable cells after hepatocyte isolation.

	<b>Body weight</b> (g)	<b>Body length</b> (cm)	<b>Number of isolated cells</b> (cells/mL)	<b>Cell viability</b> (%)
<i>O. mykiss</i> 1	216	26.5	$4.9 \times 10^6$	89
<i>O. mykiss</i> 2	228	28.4	$5.5 \times 10^6$	85
<i>O. mykiss</i> 3	189	27.5	$3.9 \times 10^6$	92

### 2.3.3. Cell culture conditions

The cells were diluted to  $0.5 \times 10^6$  cells/mL and seeded on 96-well Primaria<sup>®</sup> plates (Falcon, BD Biosciences, San Jose, California, USA) to improve cell attachment in the wells. Final density of the cells was 0.1 million cells/200  $\mu$ L (corresponding to the volume of a well). The isolated hepatocytes were incubated at 15 °C and retention of cells was observed by microscopy (Olympus CKX41 microscope, Olympus, Hamburg, Germany).

## 2.4. Exposure of hepatocytes to PCPs

### 2.4.1. General exposure conditions

Isolated hepatocytes were maintained in culture medium for two days. After 24 h of incubation half of the medium was carefully replaced by new medium, to avoid detachment of the cells from the bottom. The medium with L-glutamine used throughout this procedure was only supplemented with sodium bicarbonate solution (4.5 mM), in order to reduce possible background effects caused by the presence of antibiotics in the culture medium. AHTN, HHCB and DEP were dissolved in 5% DMSO and aliquots were stored at -22 °C. Stock solutions of VER and MK571 (dissolved in 2% DMSO) and Rho123 (dissolved in 10% DMSO) were prepared in Milli-Q water and stored at -22 °C. These aliquots were thawed directly before use and diluted in L-15 medium until the desired concentrations were reached. The obtained dilutions were adjusted by adding DMSO, to have the same concentration of solvent in each sample. For VER, MK571 and Rho123 the final concentration of DMSO in culture medium was 0.1% (v/v).

### 2.4.2. Single exposure

To determine the effect of single compounds, hepatocytes were exposed to PCPs separately. After 24 h of incubation, half of the medium from the plates designed for PCPs exposure was replaced by medium containing different concentrations of AHTN and

HHCB (0.02, 0.2, 2.3, 23.3, 200 and 1000  $\mu\text{M}$ ) and DEP (2.3, 23.3, 232.8, 2328, 20000 and 100000  $\mu\text{M}$ ), whereas half of the medium from the plates designed for inhibitor standard curves was replaced by new culture medium (plate design on **Figure 11**, Appendix I). Plates were incubated with the test compounds for 24 h to determine ABC transporter activity and cytotoxicity. The concentration of DMSO in culture medium was 0.5% (v/v). DMSO was included as a solvent with control cells. A total of three replicates were done.

#### 2.4.3. Mixture exposure

The effect of a mixture of PCPs was determined by exposing hepatocytes to a combination of two of the compounds previously used; PCPs solutions were prepared separately and posteriorly mixed inside the well. After 24 h of incubation, half of the medium was replaced by medium containing a mixture of AHTN and HHCB (0.06, 0.56, 5.6, 56, 100 and 1000  $\mu\text{M}$  of each musk) and a mixture of HHCB (0.06, 0.56, 5.6, 56, 100 and 1000  $\mu\text{M}$ ) and DEP (5.6, 56, 557, 5571, 10000 and 100000  $\mu\text{M}$ ); plate design on **Figure 12**, Appendix I. Plates were incubated for 24 h to determine ABC transporter activity. The concentration of DMSO in culture medium was 1% (v/v). DMSO was included as a solvent with control cells. A total of three replicates were done.

### 2.5. Cytotoxicity testing

Fluorescent dyes were used as a non-invasive method to evaluate cell viability of primary hepatocyte cultures. Schreer *et al.* (2005) described the combined AB/CFDA-AM assay as a suitable tool for *in vitro* measurements of cell viability in primary rainbow trout hepatocytes. This method, together with mBCI, was also successfully used on plaice, long rough dab and Atlantic cod primary hepatocytes (Ellesat *et al.*, 2011). Therefore, AB, CFDA-AM and mBCI were used as a measure of cell metabolic activity, cell membrane integrity and amount of reduced glutathione (GSH), respectively. In living cells, AB is reduced by mitochondrial reductases into resorufin, a water soluble and fluorescent dye; its presence represents a functional metabolic activity. In case of an impaired metabolic activity, the amount of resorufin in the cells decreases, which results in lower fluorescence levels. CFDA-AM, a membrane permeable, apolar and non-fluorescent dye, is hydrolysed by cytosolic esterases into 5-carboxyfluorescein (CF), a polar fluorescent dye. CF is retained in the cells, which allows the measurement of cell membrane integrity. When enzymatic activity is compromised, the amount of CF in the cells decreases leading to lower fluorescence levels; this represents a loss of membrane integrity. mBCI enters cells and forms a fluorescent adduct with the water soluble substrate GSH, which is a product

of cell defense against reactive oxygen species. This reaction is considered a measurement of oxidative stress and it is catalyzed by glutathione S-transferase (GST; Kamencic *et al.*, 2010). The measured fluorescence reflects the GSH content; fluorescence will be greater the more GSH is present in the cells. The cytotoxicity measurements were performed according to the protocol described by Ellesat *et al.* (2011). All medium was removed from the cell cultures and replaced by 100  $\mu$ L of Tris-buffer (**Table 11**, Appendix I) containing 5% AB, 4  $\mu$ M CFDA-AM and 275  $\mu$ M mBCI. Cells were incubated in the dark for 30 min on an orbital shaker at room temperature. Fluorescence was measured at excitation/emission wavelengths of 530 nm/590 nm (AB), 485 nm/530 nm (CFDA-AM) and 360 nm/460 nm (mBCI) with a Synergy Mx microplate reader (BioTek Instruments, Winooski, Vermont, USA). These measurements could be done simultaneously since the fluorescent probes can be detected at different wavelength pairs. Sensitivity of the instrument was set to 80%. To measure autofluorescence of untreated hepatocytes, the cells were maintained in culture medium alone. CFDA-AM (4 mM) and mBCI (50 mM) stock solutions were prepared in DMSO and stored at  $-22$  °C.

## 2.6. ABC transporter activity

The transporter activities in *Oncorhynchus mykiss* hepatocytes were determined by using the fluorescent ABC transporter substrate rhodamine 123. The inhibitory potential of PCPs was compared with the inhibitory effect of the transporter inhibitors MK571 (which mainly targets ABCC transporters) and VER (general inhibitor, but thought to inhibit ABCB1; Faria *et al.*, 2011). Based on the findings of Zaja *et al.* (2008) and Ferreira *et al.* (2014), increasing concentrations (0.1, 0.3, 1.7, 8.5, 10 and 50  $\mu$ M) of the inhibitors MK571 and VER were selected to perform standard curves. After 48 h of incubation, half of the culture medium (100  $\mu$ L) was removed and 50  $\mu$ L of medium containing the model inhibitors MK571 and VER was added. Hepatocytes were incubated for 5 min at room temperature. After this pre-incubation period, 50  $\mu$ L of medium containing the model substrate Rho123 was added to the wells. From the wells containing cells previously exposed to PCPs, only 50  $\mu$ L of culture medium was removed and replaced by medium containing the substrate Rho123. Final concentration of Rho123 was 1  $\mu$ M. The cells were incubated in the dark for 2 h on an orbital shaker at room temperature. After the incubation period the cells were washed with 200  $\mu$ L sterile PBS (pH 7.4, 310 mOsm). Cells were lysed by adding 200  $\mu$ L of 0.5% Triton X-100 in PBS and subjecting them to three shaking cycles of 2 s. The accumulation level of Rho123 in the cells, which is detected by its fluorescence, can be related to the ABC transporter activity (Smital *et al.*, 2003). In the case of inhibition of transporter activity, increased levels of Rho123 will be accumulated in the cells and



fluorescence will be higher. Fluorescence was measured at 485 nm excitation and 538 nm emission with a Synergy Mx microplate reader (BioTek Instruments). Sensitivity of the instrument was set to 80%. The autofluorescence of untreated hepatocytes was measured to be used as blank.

## 2.7. Data analysis

Experiments were conducted with three fish replicates, i.e. three primary cell cultures were performed using one fish for each. As shown in the plate design (**Figure 11** and **Figure 12**, Appendix I), each treatment group consists of eight pseudo-replicates. Thus, final number of pseudo-replicates for each concentration of PCPs and inhibitors equals twenty-four. Data were plotted in a x,y graph using GraphPad Prism 6.04 (GraphPad Software, San Diego, California, USA). For the cytotoxicity assays and MXR inhibitors, data were standardized relative to control (average value). When analyzing ABC transporter activity of PCPs, data were standardized relative to the lowest and highest effect concentration (average value) of the inhibitor MK571. Experimental replicates were standardized separately. The obtained values were expressed in percentages and plotted against the logarithm of agonist concentration. The non-linear regression curve fit applied was a sigmoidal (four-parameter logistic) dose-response curve with the bottom and top values set at 0 and 100, respectively. The ABC transporter activity data obtained was further used for model prediction calculations. CA predictions of binary mixtures of PCPs were calculated as,

$$C_{mix} = \left( \frac{p_1}{c_1} + \frac{p_2}{c_2} \right)^{-1}$$

, where  $C_{mix}$  represents the concentration of the mixture, derived from the individual concentrations  $c_1$  and  $c_2$  and respective proportions  $p_1$  and  $p_2$  of the total concentration (Thorpe *et al.*, 2006). Total concentration means the sum of  $c_1$  and  $c_2$ , i.e. the combined concentration of single substance 1 and 2 given a certain effect. These values were obtained through the dose-response curve by constraining the curve fit to different  $F$  values, corresponding to  $EC_{10}$ ,  $EC_{20}$ , etc., with a total of 13 steps. IA predictions were calculated as,

$$E_{mix} = 1 - ((1 - e_1)(1 - e_2))$$

, where  $E_{mix}$  represents the percentile effect of the mixture, derived from the individual percentile effects  $e_1$  and  $e_2$  (Hadrup *et al.*, 2013).  $E_{mix}$  is represented as function of the combined concentration of substance 1 and 2. Statistical comparisons of  $EC_{50}$  values for

mixture toxicity were performed using the extra sum-of-squares F test with an  $\alpha$  error of 0.05. Results are expressed as mean  $\pm$  standard deviation (SD) with confidence intervals (CI) established at 95%.

### 3. Results

#### 3.1. Cytotoxicity testing

The effects of PCPs are presented as dose-response curves and were quantitatively estimated as concentrations able to cause effect on 50% of the exposed cells ( $EC_{50}$ ; effective concentration). The data included in this analysis corresponds to two experimental replicates ( $n = 2$ , which means 16 pseudo-replicates), since the dose-response curves obtained for the last primary cell culture deviated from the dose-response relationships of the other two replicates, leading to inconclusive results. The measured fluorescence of hepatocytes exposed to the solvent control DMSO was higher than for hepatocytes used as blank, suggesting a negative impact of DMSO on cell viability. In the data analysis, comparison of the exposure groups to the control group was done. Therefore, direct reference to the toxic effect of DMSO is not considered relevant. All individual experimental replicates can be found in Appendix II.

##### 3.1.1. Cell metabolic activity

The metabolic function of the mitochondria after 24 h of exposure of hepatocytes to PCPs is summarized in **Figure 3** and **Table 3**. The generated dose-response curves are sigmoidal and possess descending slopes. AHTN and DEP only started to show effect at  $200 \times 10^{-6}$  M and  $20 \times 10^{-3}$  M, respectively; these concentrations are extremely close to their  $EC_{50}$  values. Mitochondrial activity of hepatocytes exposed to HHCB was reduced at concentrations starting from  $2.3 \times 10^{-6}$  M and impairment of the metabolic function of 50% of the cells was observed at  $4.71 \times 10^{-6}$  M.

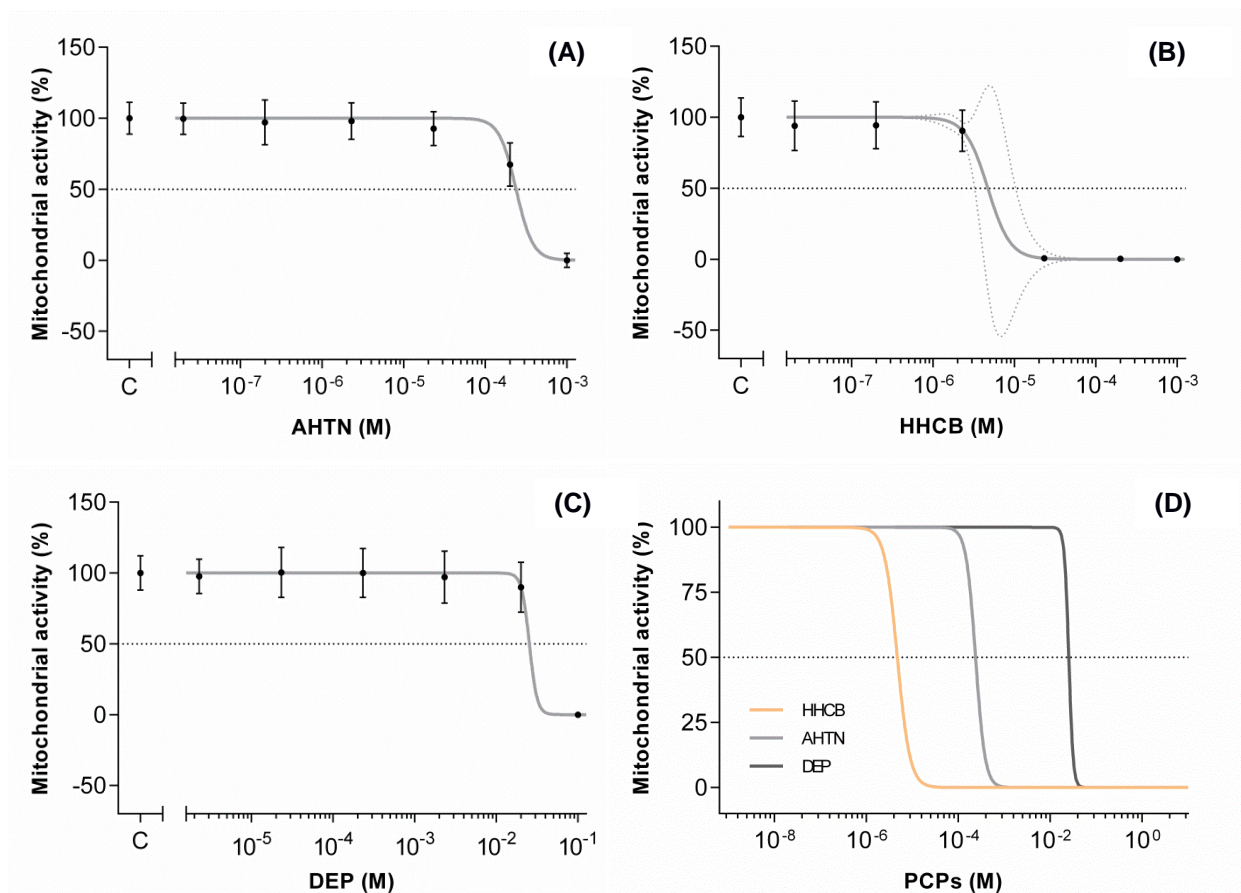


**Figure 3.** Mitochondrial activity of hepatocytes exposed to **(A)** AHTN, **(B)** HHCB, **(C)** DEP and **(D)** comparison of these three PCPs (% of control; mean  $\pm$  standard deviation;  $n = 2$ ; dotted lines: 95% confidence interval; C: control).

**Table 3.** Personal care products  $EC_{50}$  values and respective 95% confidence interval for mitochondrial activity of hepatocytes, derived from a non-linear regression curve fit.

	AHTN	HHCB	DEP
$r^2$	0.889	0.941	0.856
$EC_{50}$ (M)	$237.6 \times 10^{-6}$	$4.71 \times 10^{-6}$	$\sim 25.40 \times 10^{-3}$
$EC_{50}$ 95% CI (M)	$119.6\text{--}472.0 \times 10^{-6}$	$1.89\text{--}11.73 \times 10^{-6}$	–

### 3.1.2. Cell membrane integrity

The membrane integrity of hepatocytes after 24 h of exposure to PCPs is summarized in **Figure 4** and **Table 4**. The dose-response curves are sigmoidal for all PCPs, with a gradually decreasing slope for AHTN and HHCB. AHTN affected membrane integrity of cells at lower concentrations than mitochondrial activity; the effects were evident at

concentrations greater than  $2.3 \times 10^{-6}$  M and the  $EC_{50}$  value is approximately two times lower ( $111.40 \times 10^{-6}$ ). HHCB has a slightly lower  $EC_{50}$  for membrane integrity than for mitochondrial activity. However, higher concentrations of AHTN and HHCB are necessary to affect the membrane integrity of 100% of the cells. DEP seems to affect mitochondrial and membrane integrity of hepatocytes in a similar way, tending to induce effects on membrane integrity at lower concentrations.

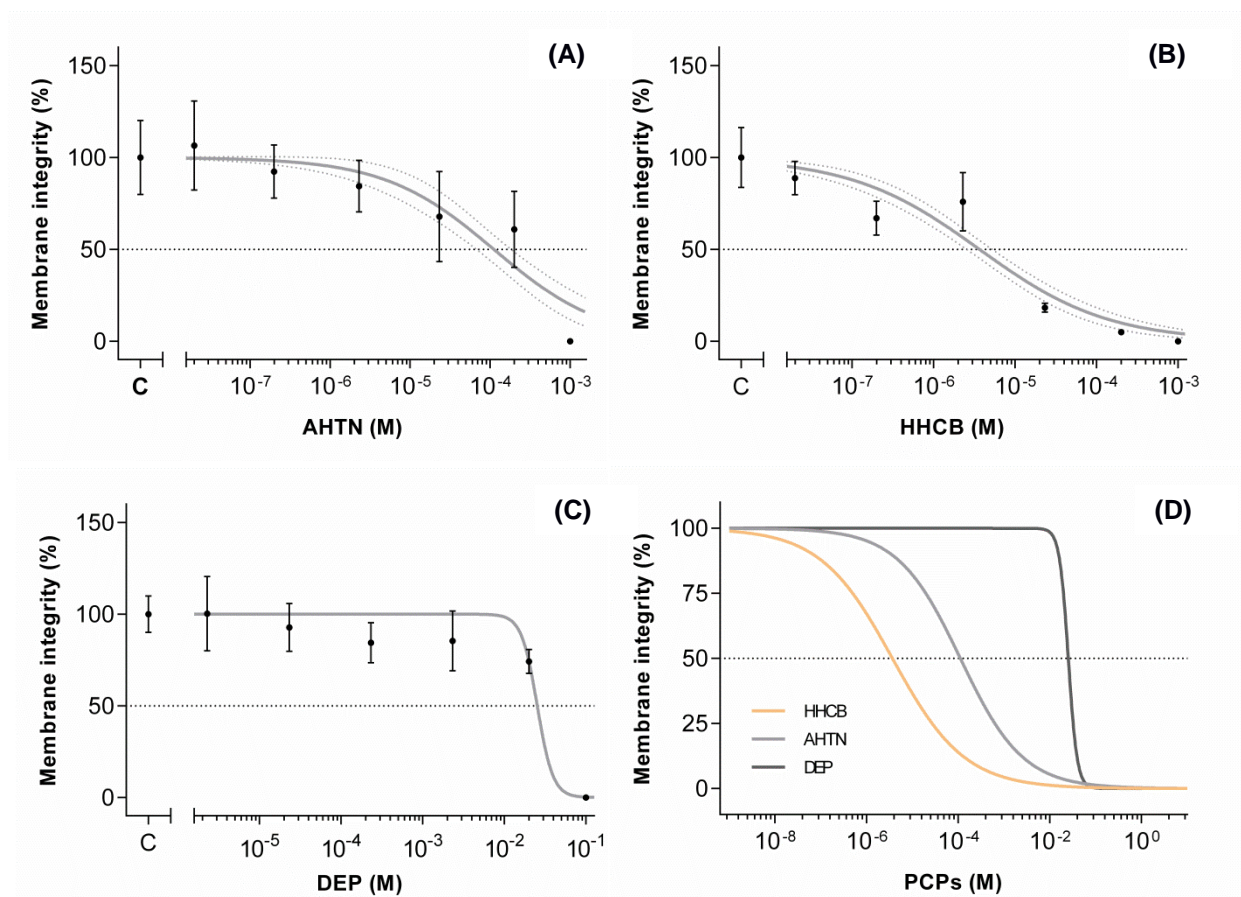


**Figure 4.** Membrane integrity of hepatocytes exposed to (A) AHTN, (B) HHCB, (C) DEP and (D) comparison of these three PCPs (% of control; mean  $\pm$  standard deviation; n = 2; dotted lines: 95% confidence interval; C: control).

**Table 4.** Personal care products  $EC_{50}$  values and respective 95% confidence interval for membrane integrity of hepatocytes, derived from a non-linear regression curve fit.

	AHTN	HHCB	DEP
$r^2$	0.679	0.853	0.811
$EC_{50}$ (M)	$111.40 \times 10^{-6}$	$3.67 \times 10^{-6}$	$25.31 \times 10^{-3}$
$EC_{50}$ 95% CI (M)	$68.69\text{--}180.60 \times 10^{-6}$	$2.57\text{--}5.23 \times 10^{-6}$	$7.32\text{--}87.48 \times 10^{-3}$



**Table 5.** Personal care products EC<sub>50</sub> values and respective 95% confidence interval for GSH content of hepatocytes, derived from a non-linear regression curve fit.

	AHTN	HHCB	DEP
r <sup>2</sup>	0.044 <sup>a</sup>	0.262	0.023 <sup>a</sup>
EC <sub>50</sub> (M)	12.23 × 10 <sup>-9</sup> <sup>a</sup>	0.35 × 10 <sup>-6</sup>	18.57 × 10 <sup>-9</sup> <sup>a</sup>
EC <sub>50</sub> 95% CI (M)	0.04–3406 × 10 <sup>-9</sup> <sup>a</sup>	0.09–1.29 × 10 <sup>-6</sup>	0.01 × 10 <sup>-12</sup> –0.04 <sup>a</sup>

<sup>a</sup> not conclusive values derived from a hypothetical non-linear regression curve fit

### 3.2. ABC transporter activity

The effects of inhibitors and PCPs on hepatocytes are quantified as dose-response curves and estimated as EC<sub>50</sub> values. The data included in this analysis corresponds to three experimental replicates (n = 3, which means 24 pseudo-replicates). The fluorescence level of hepatocytes exposed to the solvent control DMSO was higher than for hepatocytes used as blank. However, reference to the toxic effect of DMSO is not considered relevant, since exposure groups are directly compared to the control group. In the figures, the concentrations of PCPs presented in red were excluded from the non-linear regression curve fit, since they represent unviable cells and cannot be considered for this parameter. All individual experimental replicates can be found in Appendix II.

#### 3.2.1. Experimental results

The ABC transporter activity of hepatocytes, after 24 h of exposure to inhibitors and PCPs as single compounds or binary mixtures, are summarized in this sub-section. The generated dose-response curves for VER and MK571 are sigmoidal and, considering the EC<sub>50</sub> values, they seem to have a similar inhibitory potential (**Figure 6** and **Table 6**). However, the individual experimental replicates for VER were not consistent (**Figure 22**, Appendix II); the first replicate was excluded from the data set, since experimental errors occurred which resulted in unknown concentrations of VER; the dose-response curve for the second replicate was non-sigmoidal with a shallow slope. For this reason, MK571 was selected as positive control and used in further data analysis.

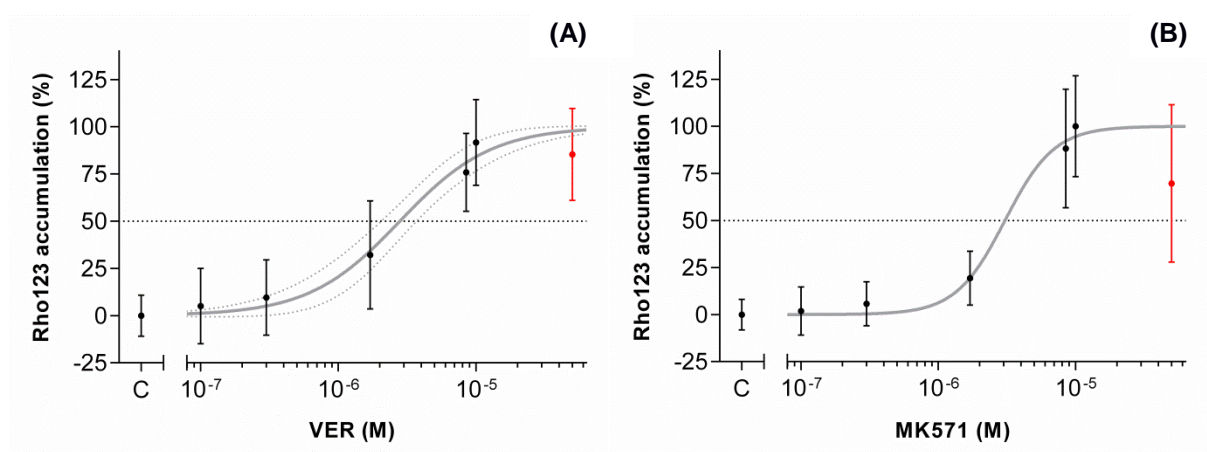


**Figure 6.** Rho123 accumulation on hepatocytes exposed to the inhibitors **(A)** VER and **(B)** MK571 (% of control; mean  $\pm$  standard deviation;  $n = 2$  for VER;  $n = 3$  for MK571; dotted lines: 95% confidence interval; C: control; red error bars: concentrations excluded from the non-linear regression curve fit).

**Table 6.** Inhibitors  $EC_{50}$  values and respective 95% confidence interval for rhodamine 123 accumulation on hepatocytes, derived from a non-linear regression curve fit.

	VER	MK571
$r^2$	0.704	0.800
$EC_{50}$ (M)	$2.80 \times 10^{-6}$	$3.06 \times 10^{-6}$
$EC_{50}$ 95% CI (M)	$2.10\text{--}3.73 \times 10^{-6}$	$0.97\text{--}9.70 \times 10^{-6}$

The dose-response curves of hepatocytes exposed to single PCPs are sigmoidal (**Figure 7**). The percentage of Rho123 accumulation in the cells was higher as the concentration increased. However, at concentrations ranging between  $200\text{--}1000 \times 10^{-6}$  M for AHTN,  $23.3\text{--}1000 \times 10^{-6}$  M for HHCb and at  $20 \times 10^{-3}$  M for DEP, the PCPs were too toxic to the cells, which resulted in a drastic decrease of the Rho123 levels. In accordance with the results obtained for cytotoxicity testing, the highest toxic effect was generated in the presence of HHCb. Despite of DEP showing higher negative effects than AHTN at low concentrations, the  $EC_{50}$  values proved that AHTN ( $32.73 \times 10^{-6}$  M) is more toxic than DEP ( $0.13 \times 10^{-3}$  M; **Table 7**).



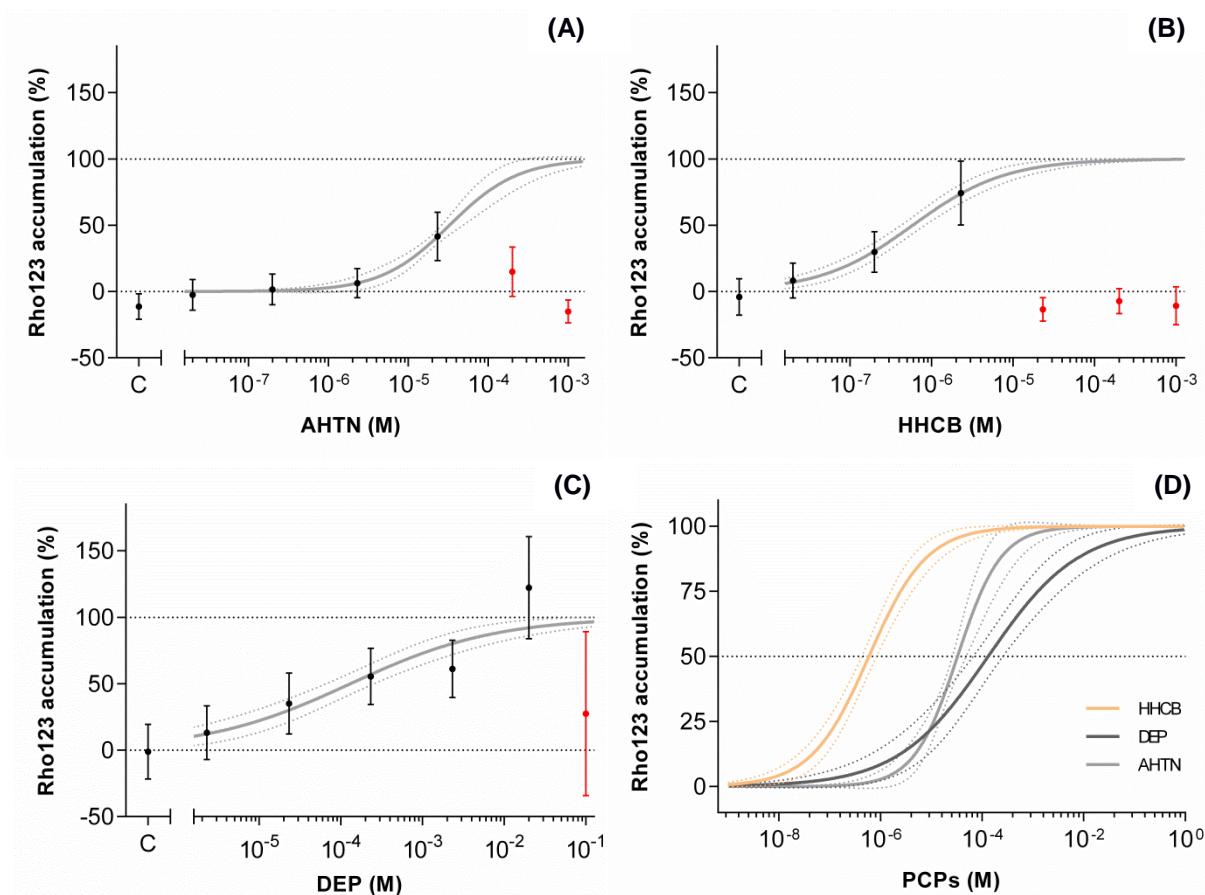


**Figure 7.** Rho123 accumulation on hepatocytes exposed to **(A)** AHTN, **(B)** HHCB, **(C)** DEP and **(D)** comparison of these three PCPs (% of MK571; mean  $\pm$  standard deviation;  $n = 3$ ; dotted lines: 95% confidence interval; C: control; red error bars: concentrations excluded from the non-linear regression curve fit).

**Table 7.** Personal care products  $EC_{50}$  values and respective 95% confidence interval for rhodamine 123 accumulation on hepatocytes, derived from a non-linear regression curve fit.

	AHTN	HHCB	DEP
$r^2$	0.634	0.703	0.544
$EC_{50}$ (M)	$32.73 \times 10^{-6}$	$0.59 \times 10^{-6}$	$0.13 \times 10^{-3}$
$EC_{50}$ 95% CI (M)	$24.65\text{--}43.45 \times 10^{-6}$	$0.42\text{--}0.82 \times 10^{-6}$	$0.07\text{--}0.25 \times 10^{-3}$

Hepatocytes exposed to binary mixtures of PCPs present a monotonous dose-response relationship (**Figure 8**). In the same manner as the single PCPs, from a certain concentration, the joint effect of PCPs is too high and the measured level of Rho123 in the cells drops. The combined effect of AHTN and HHCB on Rho123 accumulation is

intermediate compared to the single compound effects. Contrariwise, the combined effect of HHCB and DEP is lower than the effect of the single compounds.

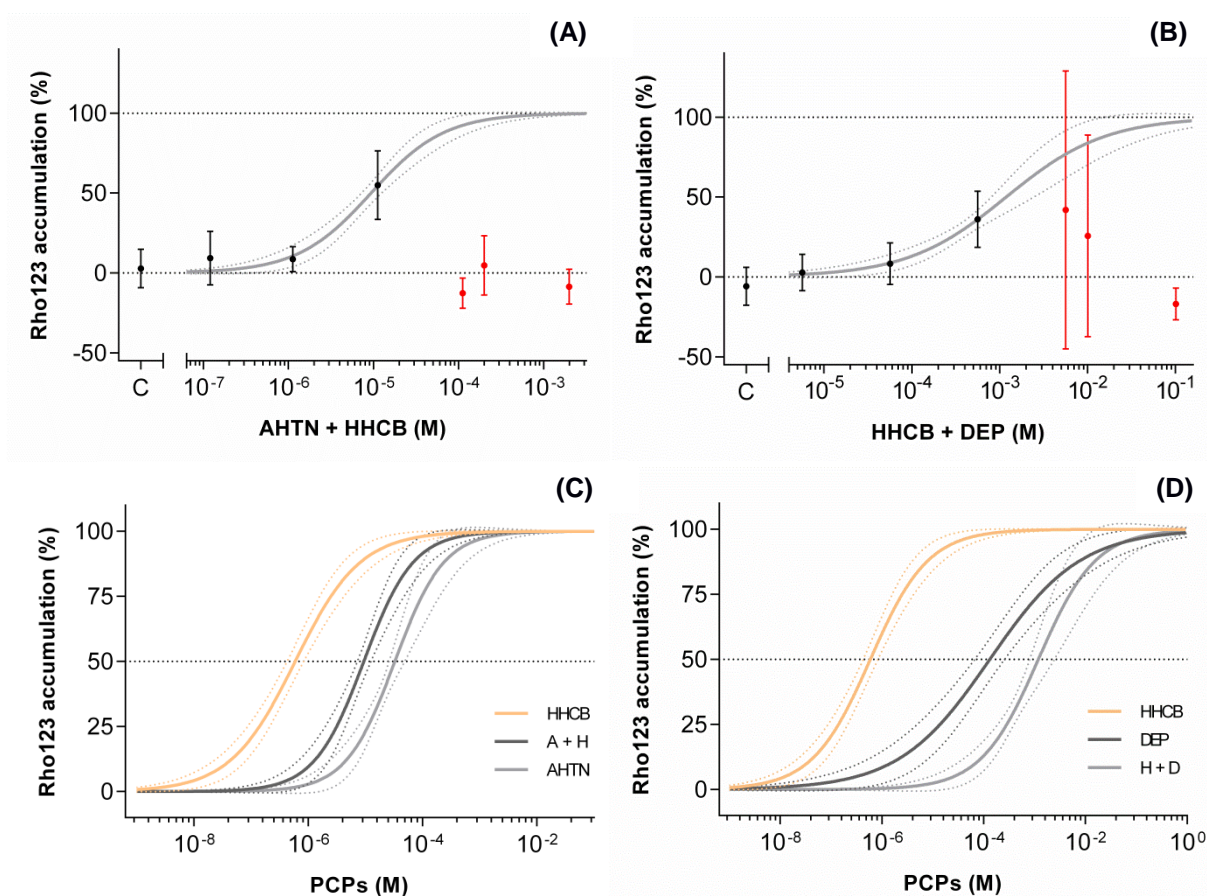


**Figure 8.** Rho123 accumulation on hepatocytes exposed to a mixture of **(A)** AHTN and HHCB **(B)** HHCB and DEP and **(C)** comparison of individual and mixed AHTN and HHCB and **(D)** individual and mixed HHCB and DEP (% of MK571; mean  $\pm$  standard deviation;  $n = 3$ ; dotted lines: 95% confidence interval; C: control; red error bars: concentrations excluded from the non-linear regression curve fit).

### 3.2.2. Model predictions

The monotonous dose-response relationships of the CA and IA models were in agreement with the experimental relationships for hepatocytes exposed to PCPs; binary mixtures of these chemicals decrease the activity of ABC transporters as their concentration increases. The CA predictions for the joint effects of AHTN and HHCB are closer to the experimental results than the respective predictions for HHCB and DEP (**Figure 9**). However, the CA model deviates from the experimental  $EC_{50}$  values from both binary mixtures; the CA model predicts approximately two times lower effects for the

mixture of AHTN and HHCB (values on **Table 8**) and approximately eighteen times higher effects for the mixture of HHCB and DEP (values on **Table 9**). For the later binary mixture, there is a significant difference between the experimental and predicted  $EC_{50}$  values ( $p < 0.0001$ ). Contrariwise, AHTN and HHCB experimental  $EC_{50}$  does not differ significantly from the predicted CA model value ( $p = 0.0608$ ).

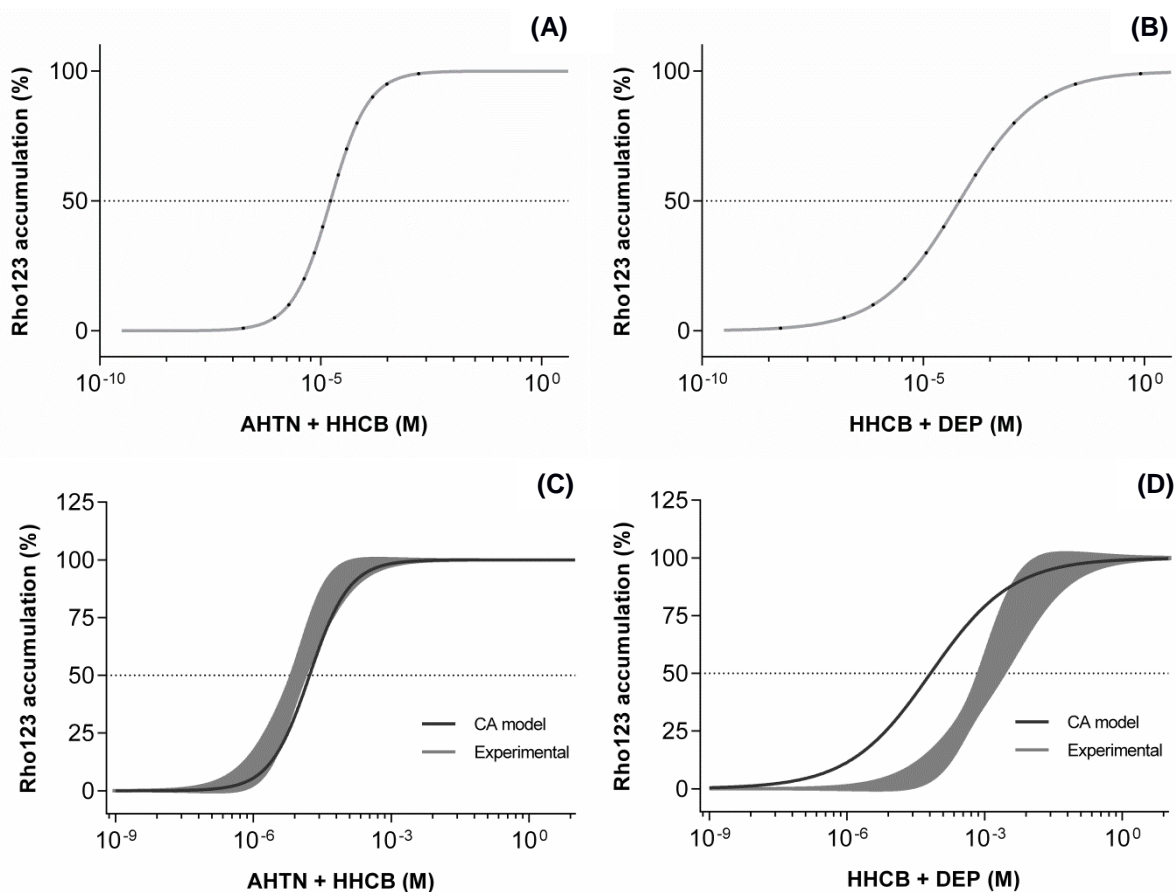


**Figure 9.** CA model predictions of Rho123 accumulation on hepatocytes exposed to a mixture of **(A)** AHTN and HHCB **(B)** HHCB and DEP and **(C)** comparison of AHTN and HHCB experimental data with the model predictions and **(D)** HHCB and DEP experimental data with the model predictions ( $n = 3$  for the experimental data; shade: 95% confidence interval).

The IA model predictions deviate from the observed effects of both binary mixtures; higher negative effects on the activity of ABC transporters are expected (**Figure 10**). However, the predicted  $EC_{50}$  value of  $1.10 \times 10^{-6}$  M for the joint effects of AHTN and HHCB is much closer to its observed  $EC_{50}$  of  $9.36 \times 10^{-6}$  M than the respective predictions for the joint effects of HHCB and DEP (values on **Table 9**). Likewise the CA model, a significant difference between the experimental and predicted  $EC_{50}$  values for the combined effects of HHCB and DEP was observed ( $p < 0.0001$ ). Nevertheless, there are no significant

deviations between the experimental and predicted  $EC_{50}$  for the mixture of AHTN and HHCB ( $p = 0.0541$ ).

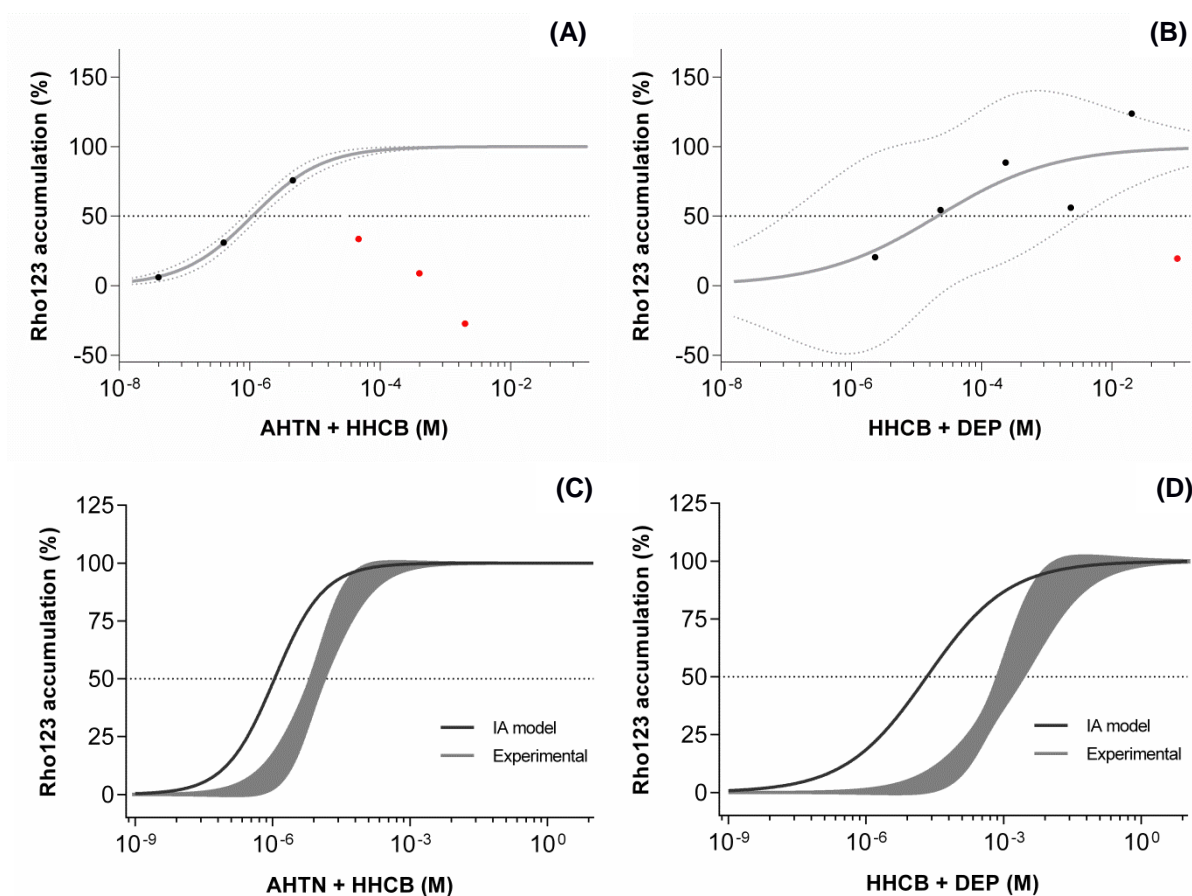


**Figure 10.** IA model predictions of Rho123 accumulation on hepatocytes exposed to a mixture of (A) AHTN and HHCB (B) HHCB and DEP and (C) comparison of AHTN and HHCB experimental data with the model predictions and (D) HHCB and DEP experimental data with the model predictions ( $n = 3$  for the experimental data; dotted lines and shade: 95% confidence interval; red dots: concentrations excluded from the non-linear regression curve fit).

**Table 8.** Experimental and predicted  $EC_{50}$  values and respective 95% confidence interval for rhodamine 123 accumulation on hepatocytes exposed to a mixture of AHTN and HHCB, derived from a non-linear regression curve fit (CA: concentration addition; IA: independent action).

	AHTN + HHCB		
	Experimental result	Model prediction	
		CA	IA
$r^2$	0.616	1.0	0.999
$EC_{50}$ (M)	$9.36 \times 10^{-6}$	$16.67 \times 10^{-6}$	$1.10 \times 10^{-6}$
$EC_{50}$ 95% CI (M)	$7.21\text{--}12.15 \times 10^{-6}$	$16.64\text{--}16.70 \times 10^{-6}$	$0.83\text{--}1.46 \times 10^{-6}$

**Table 9.** Experimental and predicted EC<sub>50</sub> values and respective 95% confidence interval for rhodamine 123 accumulation on hepatocytes exposed to a mixture of HHCB and DEP, derived from a non-linear regression curve fit (CA: concentration addition; IA: independent action).

	HHCB + DEP		
	Experimental result	Model prediction	
		CA	IA
r <sup>2</sup>	0.519	1.0	0.651
EC <sub>50</sub> (M)	1186 × 10 <sup>-6</sup>	66.09 × 10 <sup>-6</sup>	21.07 × 10 <sup>-6</sup>
EC <sub>50</sub> 95% CI (M)	712.20–1975 × 10 <sup>-6</sup>	65.94–66.24 × 10 <sup>-6</sup>	0.18–2424 × 10 <sup>-6</sup>

## 4. Discussion

### 4.1. Cytotoxicity testing

#### 4.1.1. Cell metabolic activity and membrane integrity

The cytotoxic effects of rainbow trout hepatocytes exposed to PCPs were expressed through diverse changes in cellular structure and mechanisms of action, including mitochondrial activity, membrane integrity and induction of oxidative stress. The non-linear relationships of hepatocytes exposed to PCPs demonstrate that there is a dose-dependent decrease of cellular metabolic activity and membrane integrity as the concentration of PCPs increases. Thus, exposure to increasing concentrations of these chemicals can directly or indirectly affect the electron transport chain, leading to an impairment of the metabolic function of mitochondria; indirect effects can derive from mitochondrial membrane disruption which also disrupts electron transport (Ostrander, 2000). Impairment of hepatocytes plasma membrane also occurs as the concentration of PCPs increases, which translates into a decline of total esterase activity. This decline can be explained by partial or complete lysis of hepatocytes and consequent release of esterases into the medium (*a posteriori* removed) or occurrence of changes in the cytoplasmic milieu that influence the enzyme stability or its catalytic activity (Ostrander, 2000). For the polycyclic musks, the fluorescent dye CFDA-AM seems to detect more severe effects than AB, since AHTN and HHCB affect membrane integrity of cells at lower concentrations than metabolic activity. This finding assumes that membrane disruption is affected prior to electron transport chain. However, tolerance of hepatocytes to higher concentrations of polycyclic musks seems to be greater at the level of membrane integrity than at the level of mitochondrial activity; higher concentrations of AHTN and HHCB are needed to affect total membrane integrity i.e. to produce 100% effect. Impairment of cell metabolism through exposure of rainbow trout cell lines to polycyclic musks was observed in previous studies. Through mitochondrial membrane permeabilization (MMP) testing, Randelli *et al.* (2011) suggest that AHTN induces early apoptosis in RTG-2 cells, with significant effects at 30 ng/mL (corresponding to 0.12  $\mu$ M). In RTL-W1 cells, Schnell *et al.* (2009) concluded that AHTN diminishes energy metabolism and decreases membrane integrity at the same concentration (0.12  $\mu$ M) and HHCB reveals significant cytotoxicity at 1.2  $\mu$ M. These findings are not in accordance with the results obtained in the present study, since polycyclic musks only elicit cytotoxic effects at higher concentrations and HHCB showed to be more toxic for rainbow trout hepatocytes than AHTN. According to the experimental results (**Table 3** and **Table 4**), the 50% effect on hepatocytes metabolic activity was recorded at 237.6  $\mu$ M (AHTN) and 4.71  $\mu$ M (HHCB), whereas the membrane

integrity of 50% of the cells was impaired at 111.4  $\mu\text{M}$  (AHTN) and 3.67  $\mu\text{M}$  (HHCB). The difference in the order of magnitude between previous studies and the results obtained in the present work suggests that rainbow trout primary hepatocytes are a less sensitive model for *in vitro* cytotoxicity testing than cell lines. In relation to DEP, the observed toxic effects of this compound are much lower than for polycyclic musks ( $\text{EC}_{50} \sim 25 \text{ mM}$ ), which may be due to lower lipophilicity of this compound ( $\log K_{ow}$  of 2.47) in comparison to polycyclic musks ( $\log K_{ow}$  of 5.7–5.9).

#### 4.1.2. Oxidative stress

Exposure of *O. mykiss* hepatocytes to certain concentrations of PCPs seems to elicit oxidative stress; the cellular GSH level was reduced which implies GSH conjugation with subsequent GSSG formation, leading to a lower intracellular GSH/GSSG ratio and subsequent oxidative stress. The response caused and the degree of toxicity depends on the compound in question, since HHCB seems to elicit a different dose-dependent pattern as AHTN and DEP. In the presence of HHCB at low concentration ranges (0.02–2.3  $\mu\text{M}$ ), hepatocytes seem to be able to cope with the formation of ROS and prevent oxidative damage; a dose-dependent increase in cellular GSH level indicates activation of antioxidant defenses. However, at higher concentrations of HHCB the cellular GSH level drops, which may suggest cell death through oxidative stress or other underlying mechanisms. Through the cellular morphology under microscopic observation, it was possible to observe that certain PCPs concentrations can cause mortality to hepatocytes. Chen *et al.* (2012) showed that fish exposed to simulated urban runoff, although being involved in oxidative stress, might be protected against the presence of HHCB through induction of antioxidant enzymes; verified for concentration ranges of 0.15–150  $\mu\text{g/L}$  i.e. 0.00058–0.58  $\mu\text{M}$ .

When evaluating the effects caused by the exposure of hepatocytes to AHTN and DEP, the phenomenon of hormesis seems to occur, since the dose-response relationships follow an inverted U-shaped pattern (i.e. increase at low concentrations followed by decrease at high concentrations). Hormesis is considered an “overcompensation to a disruption in homeostasis” (Calabrese, 1997). Low concentrations of these PCPs induce a stimulatory response in rainbow trout hepatocytes, which translates into an increment of cellular GSH levels. This stimulatory effect is around 40-60% greater than the control and likely is a protective mechanism against oxidative stress (Calabrese, 1997). However, at higher PCPs concentrations this over-compensatory response gives rise to an exhaustion of the cellular defense mechanisms, which translates into a decline of the GSH levels of hepatocytes. Thus, hepatocytes might be protected against damages caused by oxidative

stress at concentration ranges of 0.02–23.3  $\mu\text{M}$  for AHTN and 2.3–20000  $\mu\text{M}$  for DEP. Nevertheless, exposure to high concentrations of these PCPs may cause cell death due to the presence of excessive intracellular ROS, as previously suggested for other models. For example, in *Paralichthys olivaceus* liver the levels of GSH, GPx and GR increase after intraperitoneal injection of DEP (900 mg/kg for 3 days) indicating induction of antioxidant enzymes probably to cope with oxidative stress caused by the substance (Kang *et al.*, 2010). Zhang (2014) concluded that exposure of carp to DEP (0.5–8 mg/L; 2.3–36  $\mu\text{M}$ ) initially increases the activity of GPx which decreases at higher concentrations; this can compromise the antioxidant defense system. Additionally, DEP induced cell membrane lipid peroxidation resulting in cell damage, as indicated by the results from Zhang (2014). In contrast Zheng *et al.* (2013) showed that *Carassius auratus* liver after intraperitoneal injection of DEP (10 mg/kg for 10 days) presented lower GPx levels, which may indicate exhaustion of the antioxidant system and consequent accumulation of ROS. This inconsistency between results might be due to differences in dose and exposure time. As previously stated, membrane disruption seems to be affected prior to electron transport chain. Since xenobiotics interacting with the electron transport can trigger oxidative stress, it is likely that this cellular response occurs last. However, it is unclear if this is the correct sequence of events or if oxidative stress presents the most severe effects and causes impairment of hepatocytes plasma membrane.

## 4.2. ABC transporter activity

### 4.2.1. Experimental results

The increasing intracellular accumulation of Rho123 (**Figure 6**, **Figure 7** and **Figure 8**) indicates transporter activity reduction and subsequent MXR inhibition. Hepatocytes follow a dose-dependent increase in Rho123 accumulation as the concentration of inhibitors and PCPs increases, which is in agreement with the findings of Smital *et al.* (2004), Luckenbach & Epel (2005); only DEP at 20000  $\mu\text{M}$  seems to induce a greater effect on hepatocytes Rho123 accumulation than the model inhibitor. Findings of Smital *et al.* (2004) and Luckenbach & Epel (2005) demonstrate significant increase in rhodamine B accumulation in *Mytilus californianus* gills exposed to synthetic musk fragrances, including AHTN and HHCB. Considering this, PCPs seem to be responsible for the inhibition of efflux transporters (i.e. to impair the MXR defense system against intracellular accumulation of xenobiotics). Furthermore, the potential of PCPs to block efflux transporters activity suggest that these chemicals act as chemosensitizers and compromise the elimination of other xenobiotics present in the organism. In this experiment it was not possible to determine which ABC transporter subfamilies were



affected, since hepatocytes were not simultaneously exposed to the model inhibitors VER and MK571 and to PCPs.

Inhibition of ABC transport activity was also verified for hepatocytes exposed to binary mixtures of PCPs. In the same manner as the measured cytotoxicity parameters, single HHCB elicited the most severe effects. However, when HHCB was combined with DEP, the binary mixture revealed lower toxicity than the single compounds. These results suggest that the high inhibitory potential of HHCB is not due to the presence of DEP in the commercial galaxolide solution (HHCB, 50% in DEP). Furthermore, interactions seem to occur between these two PCPs resulting in an antagonistic effect. The potential of the binary mixture of AHTN and HHCB to inhibit the MXR defense mechanism of hepatocytes was intermediate between the potential of the respective single compounds i.e., the combination of the two polycyclic musks seems to elicit a lower effect than the most toxic compound (HHCB) and a greater effect than the less toxic compound (AHTN). This suggests that indirect interactions occur when AHTN and HHCB are present in a mixture. Nevertheless, the combined effects of a mixture of polycyclic musks are much severe than the combined effects of galaxolide and diethyl phthalate.

#### 4.2.2. Model predictions

The PCPs used in this study are considered endocrine disruptors belonging to two different categories: AHTN and HHCB have antiestrogenic effects and DEP is considered antiandrogenic (Witorsch & Thomas, 2010). The dose-response relationship of the binary mixture consisting of polycyclic musks behaves according to the CA model predictions, since experimental and predicted  $EC_{50}$  values were not significantly different, meaning that the mixture of AHTN and HHCB induced additive effects on *O. mykiss* hepatocytes. Luckenbach & Epel (2005) and Schnell *et al.* (2009) stated the same findings i.e. that the MXR inhibitory potential of combined musks is additive. Additionally, Kortenkamp *et al.* (2007) showed that mixture effects of endocrine disruptors belonging to the same category can be predicted through the CA model. This confirms that CA is a good reference model for toxicity predictions of chemicals sharing the same mechanism of action. In contrast, the results obtained for the HHCB/DEP mixture indicate that the combined effects induced by these two PCPs do not behave according to the CA and IA model predictions, since significant differences were observed between experimental and predicted  $EC_{50}$  values. Deviations from these predictions can be interpreted as interactions which in this case are antagonistic, since the combined effects of these two PCPs were lower than expected. This may be due to the different mechanisms of toxic action of the tested substances (HHCB has an antiestrogenic effect, while DEP has an

antiandrogenic action; Witorsch & Thomas, 2010). Since CA and IA models predictions were similar, both models seem to be suitable to assess combined effects of substances with diverse modes of action.

### **4.3. Assessment of primary hepatocyte viability**

Hepatocytes of rainbow trout were successfully isolated using a two-step perfusion and maintained as primary cell cultures. Before starting a culture, the cell viability was high, with values greater than 80% and hepatocytes with a round shape. However, during the incubation period the viability of cells was declining and the density was lower than expected (cell sometimes were less than 70% confluent). In some cases, it was possible to observe that hepatocytes were entering in a cell death process because some hepatocytes were starting to acquire a different shape, to shrink and to agglomerate. Although being natural that hepatocytes in a culture de-differentiate and consequently diverse morphological and structural changes occur, this fact is not sufficient to explain the observed low density of the cell monolayer (Soldatow *et al.*, 2013). The isolation technique implied the action of an enzyme to disaggregate the tissue followed by mechanical disruption; therefore, bacterial collagenase (type VII) was selected to perform an *in situ* liver perfusion. The enzymatic digestion is critical to the establishment of functional cultures; its performance can be affected by the enzyme type and respective concentration in solution, exposure time and circulation conditions. The experimental design could have failed in this step and no digestion occurred, since previous primary fish hepatocyte cultures were successfully established by using collagenase type IV (Ellesat *et al.*, 2010 & 2011). Furthermore, exposure of liver cells to the perfusion buffer containing collagenase could have been too long for the size of the fish or too located, since *in situ* perfusion reduces the recirculation level of the solution (Segner, 1998). Taking into account observations made throughout this experiment, shorter periods of exposure to collagenase (maximum 10 min) are suggested for juvenile rainbow trout; removal of the liver between the first and the second perfusion step could be a solution to facilitate recirculation and overcome local loss of cell viability. In order to improve culture conditions and avoid losses in cell functionality over time, more attention should be given to parameters that influence the physiological state of cells (Hodne *et al.*, 2012). For instance, osmotic stress can be induced if osmolality of culture mediums are below the plasma osmolality of fish (Hodne *et al.*, 2012). Even though osmolality of the medium and solutions were adjusted to physiological values, adjustment in pH and temperature should be better monitored. The pH of the solutions and medium used throughout the hepatocyte isolation and culture were ranging between 7.5–7.6. Nevertheless, these measurements

were done before the sterile filtration and incubation; factors such as rise of pH after filtration and influence of CO<sub>2</sub> level and temperature in culture were not considered. Therefore, the initial measured pH value is not a good indicator of the final value in culture. The pH in culture should be similar to the plasma pH of the fish (in teleosts, it ranges between 7.7–7.9; Hodne *et al.*, 2012). Regarding the temperature, 15 °C was proven to be adequate in the maintenance of rainbow trout hepatocytes (Ellesat *et al.*, 2010). However, Segner (1998) showed that cell viability over time was greater for *O. mykiss* hepatocytes maintained at 10 °C than at 14 °C. These findings suggest that temperature of cell cultures should be closer to the water conditions of the environment where fish was maintained before being sacrificed. Culture conditions should be as close as possible to the natural environment values of the organism to avoid additional stress factors and extend cell culture longevity.

## 5. Conclusions

Exposure of *O. mykiss* hepatocytes to three common personal care products, including AHTN, HHCB and DEP revealed to cause toxic effects. Increasing concentrations of PCPs affected the metabolic function of mitochondria and caused cellular membrane disruption, following a dose-response relationship. At high PCPs concentrations, the electron transport chain impairment and consequent mitochondrial dysfunction can result in oxidative stress. At low PCPs concentrations, hepatocytes seem to cope with the presence of ROS through induction of the antioxidant defense system. These findings corroborate the first hypothesis, namely that exposure to PCPs causes a dose-dependent cytotoxic effect on *O. mykiss* hepatocytes. However, for the oxidative stress parameter, AHTN and DEP did not follow a sigmoidal dose-response relationship; these substances seem to act in accordance with the hormesis dose-response phenomenon.

PCPs decreased the ABC transporter activity of hepatocytes as the concentration increased i.e. in a dose-dependent manner. Thus, the second hypothesis was verified, namely that there is a dose-dependent decrease in ABC transporter activity of *O. mykiss* hepatocytes after exposure to single PCPs. This means that these substances inhibit the MXR defense mechanism of hepatocytes and intracellular accumulation of xenobiotics can occur. Consequently, PCPs can act as chemosensitizers and in its presence, organisms become more susceptible to exposure to other xenobiotics present in the environment.

The results of the present study also indicated toxicological interactions between the binary mixtures of PCPs tested at the ABC transporter activity level, thus corroborating the third hypothesis. The combined effects of the two tested polycyclic musks were in agreement with CA model predictions. This means that the toxic effects induced on the ABC transporter activity, by the simultaneous exposure of hepatocytes to AHTN and HHCB, were additive. The HHCB/DEP binary mixture effects were neither in accordance with CA nor with IA model predictions; the toxicity of the mixture was lower than predicted which indicates that interactions occur between these two PCPs i.e. the HHCB/DEP mixture effects on ABC transporter activity were antagonistic.

Polycyclic musks and diethyl phthalate are present in surface waters at much lower levels than the concentration ranges tested in this experiment. However, it is important to take into consideration that these chemicals can accumulate in the aquatic system and adsorb to sediments, increasing its concentration in the environment. Therefore, these PCPs are available to aquatic organisms and can trigger mechanism of toxicity. Nevertheless, it is

important to evaluate the toxic effects of PCPs at environmental relevant concentrations and perform short and long-term exposure experiments with aquatic organisms. Thus, acute and chronic effects can be assessed and, at the same time, the recovery potential of these organisms can be evaluated. Further research is needed to better understand the mechanism involved in oxidative stress and to determine the presence and expression of ABC proteins in hepatocytes, since isolation and culture of hepatocytes can affect the expression profile of these transporters. Additionally, it is important to obtain a broad view of the consequences of such exposures and be able to understand them at a population and ecosystem level.

## References

- Al-Jandal, N. J., & Wilson, R. W. (2011). A comparison of osmoregulatory responses in plasma and tissues of rainbow trout *Oncorhynchus mykiss* following acute salinity challenges. *Comparative Biochemistry and Physiology Part A: Molecular & Integrative Physiology* 159: 175–181.
- American Chemistry Council (2014). *Phthalates: Personal Care Products*. Retrieved August 13, 2014, from American Chemistry: <http://phthalates.americanchemistry.com/Phthalates-Basics/Personal-Care-Products>.
- Ankeny, R. A., & Leonelli, S. (2011). What's so special about model organisms?. *Studies in History and Philosophy of Science* 42: 313–323.
- Baas, J., Stefanowicz, A. M., Klimek, B., Laskowski, R., & Kooijman, S. A. (2010). Model-based experimental design for assessing effects of mixtures of chemicals. *Environmental Pollution* 158: 115–120.
- Backhaus, T., & Faust, M. (2012). Predictive environmental risk assessment of chemical mixtures: a conceptual framework. *Environmental Science and Technology* 46: 2564–2573.
- Balk, F., & Ford, R. A. (1999). Environmental risk assessment for the polycyclic musks AHTN and HHCB in the EU: I. Fate and exposure assessment. *Toxicology Letters* 111: 57–79.
- Bester, K. (2009). Analysis of musk fragrances in environmental samples. *Journal of Chromatography A* 1216: 470–480.
- Brausch, J. M., & Rand, G. M. (2011). A review of personal care products in the aquatic environment: environmental concentrations and toxicity. *Chemosphere* 82: 1518–1532.
- Calabrese, E. J. (1999). Evidence that hormesis represents an “overcompensation” response to a disruption in homeostasis. *Ecotoxicology and Environmental Safety*, 42: 135–137.
- Cedergreen, N., Abbaspoor, M., Sørensen, H., & Streibig, J. C. (2007). Is mixture toxicity measured on a biomarker indicative of what happens on a population level? A study with *Lemna minor*. *Ecotoxicology and Environmental Safety* 67: 323–332.
- Cedergreen, N., Christensen, A. M., Kamper, A., Kudsk, P., Mathiassen, S. K., Streibig, J. C., & Sørensen, H. (2008). A review of independent action compared to concentration addition as reference models for mixtures of compounds with

- different molecular target sites. *Environmental Toxicology and Chemistry* 27: 1621–1632.
- Chen, F., Gao, J., & Zhou, Q. (2012). Toxicity assessment of simulated urban runoff containing polycyclic musks and cadmium in *Carassius auratus* using oxidative stress biomarkers. *Environmental Pollution* 162: 91–97.
- Choi, C. H. (2005). ABC transporters as multidrug resistance mechanisms and the development of chemosensitizers for their reversal. *Cancer Cell International* 5: 30.
- Croom, E. (2012). metabolism of xenobiotics of human environments **In:** *Progress in Molecular Biology and Translational Science*. Hardbound, D. T. (Ed.). Vol 112, 1<sup>st</sup> edition, Academic Press, Elsevier, 31–88 pp.
- Cuthbertson, L., Kos, V., & Whitfield, C. (2010). ABC transporters involved in export of cell surface glycoconjugates. *Microbiology and Molecular Biology Reviews* 74: 341–362.
- Di Giulio, R.T., & Newman, M. C. (2013). ecotoxicology **In:** *Casarett and Doull's Toxicology: The Basic Science of Poisons*. Klaassen, C. D. (Ed.). Vol. 1236, 8<sup>th</sup> edition, McGraw-Hill, New York, 1275–1303 pp.
- Duedahl-Olesen, L., Cederberg, T., Pedersen, K. H., & Højgård, A. (2005). Synthetic musk fragrances in trout from Danish fish farms and human milk. *Chemosphere* 61: 422–431.
- Ellesat, K. S., Tollefsen, K. E., Åsberg, A., Thomas, K. V., & Hylland, K. (2010). Cytotoxicity of atorvastatin and simvastatin on primary rainbow trout *Oncorhynchus mykiss* hepatocytes. *Toxicology in vitro* 24: 1610–1618.
- Ellesat, K. S., Yazdani, M., Holth, T. F., & Hylland, K. (2011). Species-dependent sensitivity to contaminants: An approach using primary hepatocyte cultures with three marine fish species. *Marine Environmental Research* 72: 216–224.
- Faria, M., Navarro, A., Luckenbach, T., Piña, B., & Barata, C. (2011). Characterization of the multixenobiotic resistance (MXR) mechanism in embryos and larvae of the zebra mussel *Dreissena polymorpha* and studies on its role in tolerance to single and mixture combinations of toxicants. *Aquatic Toxicology* 101: 78–87.
- Ferreira, M., Santos, P., Rey-Salgueiro, L., Zaja, R., Reis-Henriques, M. A., & Smital, T. (2014). The first demonstration of CYP1A and the ABC protein (s) gene expression and activity in European seabass *Dicentrarchus labrax* primary hepatocytes. *Chemosphere* 100: 152–159.

- Frei, M. (2011). *Centrifugation*. Retrieved August 13, 2014, from Sigma-Aldrich: <http://www.sigmaaldrich.com/life-science/learning-center/biofiles/biofiles-6-5.html>.
- Hadrup, N., Taxvig, C., Pedersen, M., Nellemann, C., Hass, U., & Vinggaard, A. M. (2013). Concentration addition, independent action and generalized concentration addition models for mixture effect prediction of sex hormone synthesis in vitro. *Plos One* 8: e70490.
- Harris, M. P., Henke, K., Hawkins, M. B., & Witten, P. E. (2014). Fish is Fish: the use of experimental model species to reveal causes of skeletal diversity in evolution and disease. *Journal of Applied Ichthyology* 30: 616–629.
- Higgins, C. F. (2001). ABC transporters: physiology, structure and mechanism—an overview. *Research in Microbiology* 152: 205–210.
- Hodgson, E. (2010). *A Textbook of Modern Toxicology*. 4<sup>th</sup> edition. John Wiley & Sons, Hoboken, New Jersey, 648 p.
- Hodne, K., von Krogh, K., Weltzien, F. A., Sand, O., & Haug, T. M. (2012). Optimized conditions for primary culture of pituitary cells from the Atlantic cod *Gadus morhua*. The importance of osmolality, pCO<sub>2</sub>, and pH. *General and Comparative Endocrinology* 178: 206–215.
- Hubinger, J. C. (2009). A survey of phthalate esters in consumer cosmetic products. *Journal of Cosmetic Science* 61: 457–465.
- Hutter, H. P., Wallner, P., Moshhammer, H., Hartl, W., Sattelberger, R., Lorbeer, G., & Kundi, M. (2009). Synthetic musks in blood of healthy young adults: Relationship to cosmetics use. *Science of the Total Environment* 407: 4821–4825.
- International Fragrance Association (2011). *EU Regulation Follows Fragrance Industry's Voluntary Global Ban*. Retrieved November 16, 2014, from International Fragrance Association (IFRA): [http://ifraorg.org/view\\_document.aspx?docId=22609](http://ifraorg.org/view_document.aspx?docId=22609).
- Kamencic, H., Lyon, A., Paterson, P. G., & Juurlink, B. H. (2000). Monochlorobimane fluorometric method to measure tissue glutathione. *Analytical Biochemistry* 286: 35–37.
- Kang, J. C., Jee, J. H., Koo, J. G., Keum, Y. H., Jo, S. G., & Park, K. H. (2010). Anti-oxidative status and hepatic enzymes following acute administration of diethyl phthalate in olive flounder *Paralichthys olivaceus*, a marine culture fish. *Ecotoxicology and Environmental Safety* 73: 1449–1455.



- Keppler, D. (2011). multidrug resistance proteins (MRPs, ABCs): importance for pathophysiology and drug therapy. **In:** *Drug Transporters*. Fromm, M. F. & Kim, R. B. (Eds.) 1<sup>st</sup> edition, Springer, Berlin Heidelberg, 299–323 pp.
- Kortenkamp, A. (2007). Ten years of mixing cocktails: a review of combination effects of endocrine-disrupting chemicals. *Environmental Health Perspectives* 115: 98–105.
- Lončar, J., Popović, M., Zaja, R., & Smital, T. (2010). Gene expression analysis of the ABC efflux transporters in rainbow trout (*Oncorhynchus mykiss*). *Comparative Biochemistry and Physiology Part C* 151: 209–215.
- Luckenbach, T., & Epel, D. (2005). Nitromusk and polycyclic musk compounds as long-term inhibitors of cellular xenobiotic defense systems mediated by multidrug transporters. *Environmental Health Perspectives*: 17–24.
- Nakata, H., Sasaki, H., Takemura, A., Yoshioka, M., Tanabe, S., & Kannan, K. (2007). Bioaccumulation, temporal trend, and geographical distribution of synthetic musks in the marine environment. *Environmental Science & Technology* 41: 2216–2222.
- National Research Council (2007) *Toxicity Testing in the 21st Century: A Vision and a Strategy*. 1<sup>st</sup> edition. National Academies Press, Washington, D.C., 216 p.
- Ostrander, G. K. (Ed.). (2000). *The Laboratory Fish*. 1<sup>st</sup> edition. Academic Press, Elsevier, 678 p.
- PubChem (2014). *Diethyl Phthalate*. Retrieved September 24, 2014, from PubChem, National Center for Biotechnology Information (NCBI): <https://pubchem.ncbi.nlm.nih.gov/compound/6781?from=summary>.
- PubChem (2014). *Galaxolide*. Retrieved September 24, 2014, from PubChem, National Center for Biotechnology Information (NCBI): <https://pubchem.ncbi.nlm.nih.gov/compound/91497?from=summary>.
- PubChem (2014). *Tonalid*. Retrieved September 24, 2014, from PubChem, National Center for Biotechnology Information (NCBI): <https://pubchem.ncbi.nlm.nih.gov/compound/89440?from=summary>.
- Ramirez, A. J., Brain, R. A., Usenko, S., Mottaleb, M. A., O'Donnell, J. G., Stahl, L. L., ... & Chambliss, C. K. (2009). Occurrence of pharmaceuticals and personal care products in fish: results of a national pilot study in the United States. *Environmental Toxicology and Chemistry* 28: 2587–2597.
- Randelli, E., Rossini, V., Corsi, I., Focardi, S., Fausto, A. M., Buonocore, F., & Scapigliati, G. (2011). Effects of the polycyclic ketone tonalide (AHTN) on some cell viability

- parameters and transcription of P450 and immunoregulatory genes in rainbow trout RTG-2 cells. *Toxicology in vitro* 25: 1596–1602.
- Robinson, L., & Thorn, I. (2005). *Toxicology and Ecotoxicology in Chemical Safety Assessment*. 1<sup>st</sup> edition. Blackwell Publishing Ltd, Oxford, 157 p.
- Schnell, S., Bols, N. C., Barata, C., & Porte, C. (2009). Single and combined toxicity of pharmaceuticals and personal care products (PPCPs) on the rainbow trout liver cell line RTL-W1. *Aquatic Toxicology* 93: 244–252.
- Schreer, A., Tinson, C., Sherry, J. P., & Schirmer, K. (2005). Application of Alamar blue/5-carboxyfluorescein diacetate acetoxymethyl ester as a noninvasive cell viability assay in primary hepatocytes from rainbow trout. *Analytical Biochemistry* 344: 76–85.
- Segner, H. (1998). Isolation and primary culture of teleost hepatocytes. *Comparative Biochemistry and Physiology Part A* 120: 71–81.
- Selvaraj, K. K., Sundaramoorthy, G., Ravichandran, P. K., Girijan, G. K., Sampath, S., & Ramaswamy, B. R. (2014). Phthalate esters in water and sediments of the Kaveri River, India: environmental levels and ecotoxicological evaluations. *Environmental Geochemistry and Health*: 1–14.
- Smital, T., Luckenbach, T., Sauerborn, R., Hamdoun, A. M., Vega, R. L., & Epel, D. (2004). Emerging contaminants—pesticides, PPCPs, microbial degradation products and natural substances as inhibitors of multixenobiotic defense in aquatic organisms. *Mutation Research/Fundamental and Molecular Mechanisms of Mutagenesis* 552: 101–117.
- Smital, T., Sauerborn, R., & Hackenberger, B. K. (2003). Inducibility of the P-glycoprotein transport activity in the marine mussel *Mytilus galloprovincialis* and the freshwater mussel *Dreissena polymorpha*. *Aquatic Toxicology* 65: 443–465.
- Soldatow, V. Y., LeCluyse, E. L., Griffith, L. G., & Rusyn, I. (2013). *In vitro* models for liver toxicity testing. *Toxicology Research* 2: 23–39.
- Stoddart, M. J. (Ed.). (2011). *Mammalian Cell Viability: Methods and Protocols*. 1<sup>st</sup> edition. Humana Press, Springer, 240 p.
- Thorpe, K. L., Gross-Sorokin, M., Johnson, I., Brighty, G., & Tyler, C. R. (2006). An assessment of the model of concentration addition for predicting the estrogenic activity of chemical mixtures in wastewater treatment works effluents. *Environmental Health Perspectives* 114: 90.

- Vethaak, A. D., Lahr, J., Schrap, S. M., Belfroid, A. C., Rijs, G. B., Gerritsen, A., ... & de Voogt, P. (2005). An integrated assessment of estrogenic contamination and biological effects in the aquatic environment of The Netherlands. *Chemosphere* 59: 511–524.
- Witorsch, R. J., & Thomas, J. A. (2010). Personal care products and endocrine disruption: A critical review of the literature. *Critical Reviews in Toxicology* 40: 1–30.
- Zaja, R., Munić, V., Klobučar, R. S., Ambriović-Ristov, A., & Smital, T. (2008). Cloning and molecular characterization of apical efflux transporters (ABCB1, ABCB11 and ABCC2) in rainbow trout *Oncorhynchus mykiss* hepatocytes. *Aquatic Toxicology* 90: 322–332.
- Zhang, G. (2014). Effect of diethyl phthalate on biochemical indicators of carp liver tissue. *Toxin Reviews*: 1–7.
- Zheng, Q., Feng, M., & Dai, Y. (2013). Comparative antioxidant responses in liver of *Carassius auratus* exposed to phthalates: An integrated biomarker approach. *Environmental Toxicology and Pharmacology* 36: 741–749.

## Appendix I

**Table 10.** Chemicals used throughout the experiment.

Product	Producer	Supplier	Product No.	CAS No.
1,3,4,6,7,8-Hexahydro-4,6,6,7,8,8-hexamethylcyclopenta[g]-2-benzopyran solution		Sigma-Aldrich	W520608	122-05-05
5-carboxyfluorescein diacetate acetoxymethyl ester	Invitrogen, Life technologies		C1354	124412-00-6
6-Acetyl-1,1,2,4,4,7-hexamethyltetralin		Sigma-Aldrich	W526401	21145-77-7
Alamar blue	Invitrogen, Life technologies		DAL1025	62758-13-8
Antibiotic antimycotic solution (100x), with 10000 units penicillin, 10 mg streptomycin and 25 µg amphotericin B per mL	Gibco, Life technologies		15240	
Bovine serum albumin		Sigma-Aldrich	A4503	9048-46-8
CaCl <sub>2</sub>		Sigma-Aldrich	C1016	10043-52-4
Collagenase VIII		Sigma-Aldrich	C2139	9001-12-1
Diethyl phthalate		Sigma-Aldrich	524972	84-66-2
Dimethyl sulfoxide	Amresco		231	67-68-5
Ethylene glycol tetraacetic acid		Sigma-Aldrich	E4378	67-42-5
KCl	Merck Millipore	VWR	1.04936	7447-40-7
L-15 (Leibovitz) medium with L-glutamine		Sigma-Aldrich	L4386	
MgSO <sub>4</sub> × 7H <sub>2</sub> O	Merck Millipore	VWR	1.05886	10034-99-8
MK 571 (sodium salt)	Cayman Chemical		70720	115103-85-0
Monochlorobimane		Sigma-Aldrich	69899	76421-73-3
Na <sub>2</sub> HPO <sub>4</sub>		Sigma-Aldrich	S5136	7558-79-4
NaCl	AnalaR Normapur	VWR	27810.295	7647-14-5

NaH <sub>2</sub> PO <sub>4</sub> × H <sub>2</sub> O		Sigma-Aldrich	71504	10049-21-5
NaHCO <sub>3</sub>		Sigma-Aldrich	S5761	144-55-8
Phosphate buffered saline		Sigma-Aldrich	P4417	
Rhodamine 123	Molecular Probes		R-302	62669-70-9
Sodium bicarbonate solution		Sigma-Aldrich	S8761	144-55-8
Triton X-100		Sigma-Aldrich	X100	9002-93-1
Trizma base		Sigma-Aldrich	T1503	77-86-1
Trizma hydrochloride		Sigma-Aldrich	T5941	1185-53-1
Trypan blue solution		Sigma-Aldrich	T8154	72-57-1
Verapamil hydrochloride		Sigma-Aldrich	V4629	152-11-4

**Table 11.** Composition of solutions used throughout the experiment. These solutions were sterilized by filtration (0.22 µm).

Solution	Chemical	Concentration
<b>Perfusion buffer</b> pH 7.5 310 mOsm	KCl	4.8 mM
	MgSO <sub>4</sub> × 7H <sub>2</sub> O	1.2 mM
	Na <sub>2</sub> HPO <sub>4</sub>	11 mM
	NaCl	122 mM
	NaH <sub>2</sub> PO <sub>4</sub> × H <sub>2</sub> O	3.3 mM
	NaHCO <sub>3</sub>	3.7 mM
<b>Tris-buffer</b> (50 µM) pH 7.4	Trizma base	8 µM
	Trizma hydrochloride	42 µM

	Blank	Control	AHTN or HHCB ( $\times 10^{-6}$ M)									
	1	2	3	4	5	6	7	8	9	10	11	12
A	Cells	DMSO	0.02	0.2	2.3	23.3	200	1000				
B	Cells	DMSO	0.02	0.2	2.3	23.3	200	1000				
C	Cells	DMSO	0.02	0.2	2.3	23.3	200	1000				
D	Cells	DMSO	0.02	0.2	2.3	23.3	200	1000				
E	Cells	DMSO	0.02	0.2	2.3	23.3	200	1000				
F	Cells	DMSO	0.02	0.2	2.3	23.3	200	1000				
G	Cells	DMSO	0.02	0.2	2.3	23.3	200	1000				
H	Cells	DMSO	0.02	0.2	2.3	23.3	200	1000				

	Blank	Control	DEP ( $\times 10^{-6}$ M)									
	1	2	3	4	5	6	7	8	9	10	11	12
A	Cells	DMSO	2.3	23.3	232.8	2328	20000	100000				
B	Cells	DMSO	2.3	23.3	232.8	2328	20000	100000				
C	Cells	DMSO	2.3	23.3	232.8	2328	20000	100000				
D	Cells	DMSO	2.3	23.3	232.8	2328	20000	100000				
E	Cells	DMSO	2.3	23.3	232.8	2328	20000	100000				
F	Cells	DMSO	2.3	23.3	232.8	2328	20000	100000				
G	Cells	DMSO	2.3	23.3	232.8	2328	20000	100000				
H	Cells	DMSO	2.3	23.3	232.8	2328	20000	100000				

	Blank	Control	Inhibitor ( $\times 10^{-6}$ M)									
	1	2	3	4	5	6	7	8	9	10	11	12
A	Cells	DMSO	0.1	0.3	1.7	8.5	10	50				
B	Cells	DMSO	0.1	0.3	1.7	8.5	10	50				
C	Cells	DMSO	0.1	0.3	1.7	8.5	10	50				
D	Cells	DMSO	0.1	0.3	1.7	8.5	10	50				
E	Cells	DMSO	0.1	0.3	1.7	8.5	10	50				
F	Cells	DMSO	0.1	0.3	1.7	8.5	10	50				
G	Cells	DMSO	0.1	0.3	1.7	8.5	10	50				
H	Cells	DMSO	0.1	0.3	1.7	8.5	10	50				

**Figure 11.** Plate design for *O. mykiss* hepatocytes exposed to single compounds (AHTN, HHCB and DEP) and inhibitors (VER and MK571). Blank corresponds to wells only with cells, control corresponds to cells exposed to the solvent control DMSO and the remaining wells correspond to cells exposed to different concentrations of personal care products or inhibitors.

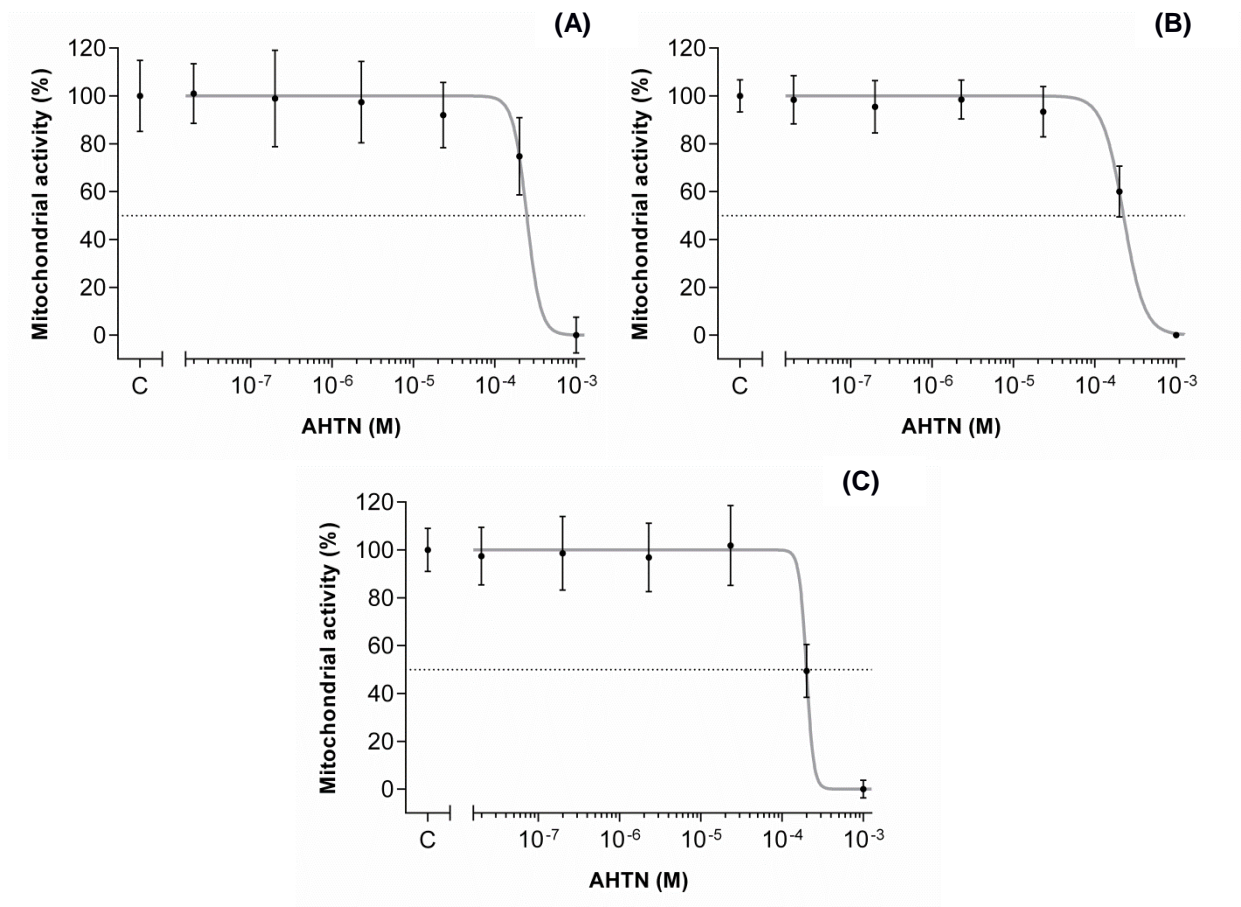
	Blank	Control	AHTN + HHCB ( $\times 10^{-6}$ M)									
	1	2	3	4	5	6	7	8	9	10	11	12
<b>A</b>	Cells	DMSO	0.06	0.56	5.6	56	100	1000				
			0.06	0.56	5.6	56	100	1000				
<b>B</b>	Cells	DMSO	0.06	0.56	5.6	56	100	1000				
			0.06	0.56	5.6	56	100	1000				
<b>C</b>	Cells	DMSO	0.06	0.56	5.6	56	100	1000				
			0.06	0.56	5.6	56	100	1000				
<b>D</b>	Cells	DMSO	0.06	0.56	5.6	56	100	1000				
			0.06	0.56	5.6	56	100	1000				
<b>E</b>	Cells	DMSO	0.06	0.56	5.6	56	100	1000				
			0.06	0.56	5.6	56	100	1000				
<b>F</b>	Cells	DMSO	0.06	0.56	5.6	56	100	1000				
			0.06	0.56	5.6	56	100	1000				
<b>G</b>	Cells	DMSO	0.06	0.56	5.6	56	100	1000				
			0.06	0.56	5.6	56	100	1000				
<b>H</b>	Cells	DMSO	0.06	0.56	5.6	56	100	1000				
			0.06	0.56	5.6	56	100	1000				

	Blank	Control	HHCB + DEP ( $\times 10^{-6}$ M)									
	1	2	3	4	5	6	7	8	9	10	11	12
<b>A</b>	Cells	DMSO	0.06	0.56	5.6	56	100	1000				
			5.6	56	557	5571	10000	100000				
<b>B</b>	Cells	DMSO	0.06	0.56	5.6	56	100	1000				
			5.6	56	557	5571	10000	100000				
<b>C</b>	Cells	DMSO	0.06	0.56	5.6	56	100	1000				
			5.6	56	557	5571	10000	100000				
<b>D</b>	Cells	DMSO	0.06	0.56	5.6	56	100	1000				
			5.6	56	557	5571	10000	100000				
<b>E</b>	Cells	DMSO	0.06	0.56	5.6	56	100	1000				
			5.6	56	557	5571	10000	100000				
<b>F</b>	Cells	DMSO	0.06	0.56	5.6	56	100	1000				
			5.6	56	557	5571	10000	100000				
<b>G</b>	Cells	DMSO	0.06	0.56	5.6	56	100	1000				
			5.6	56	557	5571	10000	100000				
<b>H</b>	Cells	DMSO	0.06	0.56	5.6	56	100	1000				
			5.6	56	557	5571	10000	100000				

**Figure 12.** Plate design for *O. mykiss* hepatocytes exposed to a personal care products mixture of AHTN/HHCB and HHCB/DEP. Blank corresponds to wells only with cells and control corresponds to cells exposed to the solvent control DMSO. The remaining wells represent cells exposed to two PCPs with different concentrations (top line, concentration of 1<sup>st</sup> compound; bottom line, concentration of 2<sup>nd</sup> compound).

## Appendix II



**Figure 13.** Mitochondrial activity of hepatocytes exposed to AHTN at the **(A)** first replicate **(B)** second replicate and **(C)** third replicate (% of control; mean  $\pm$  standard deviation; C: control).



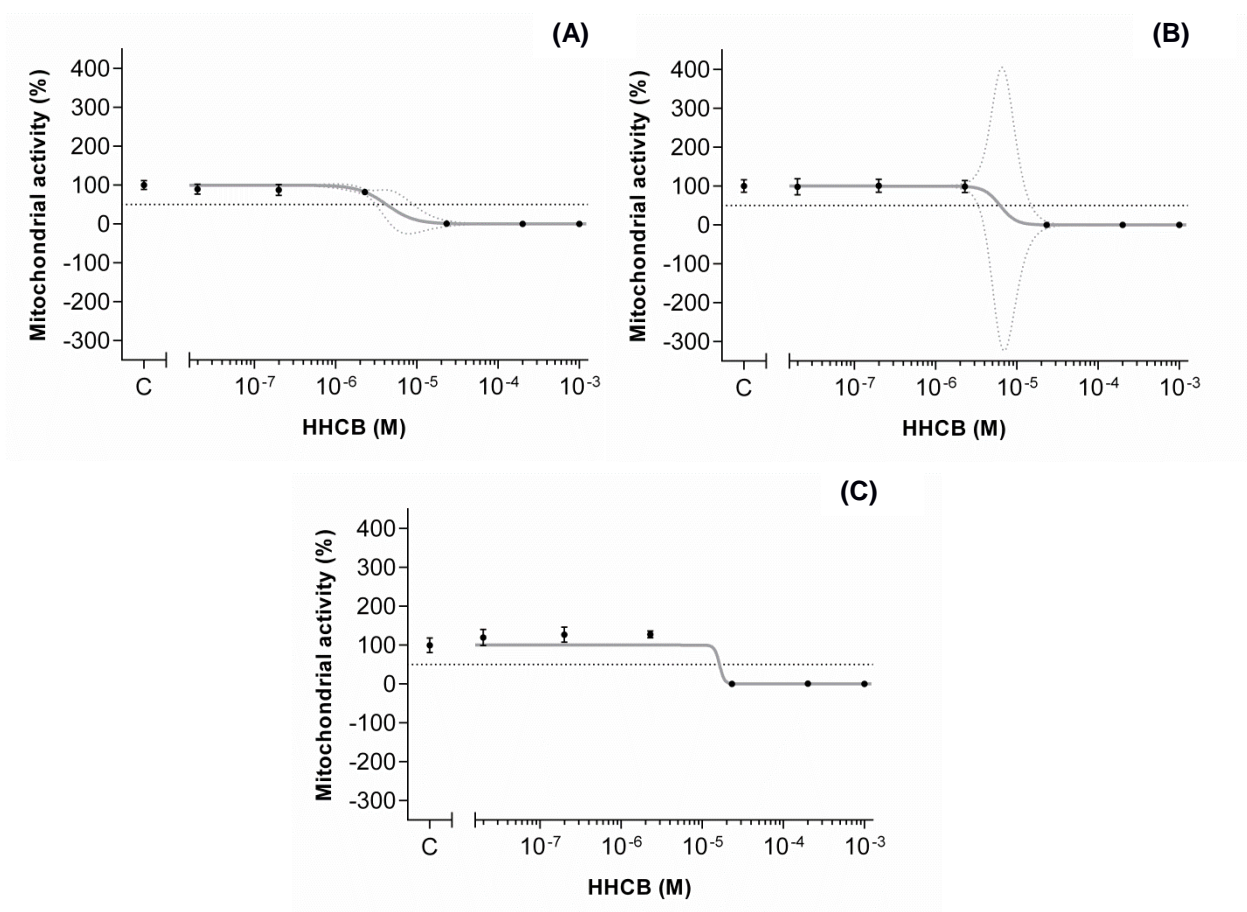


**Figure 14.** Mitochondrial activity of hepatocytes exposed to HHCB at the **(A)** first replicate **(B)** second replicate and **(C)** third replicate (% of control; mean  $\pm$  standard deviation; dotted lines: 95% confidence interval; C: control).

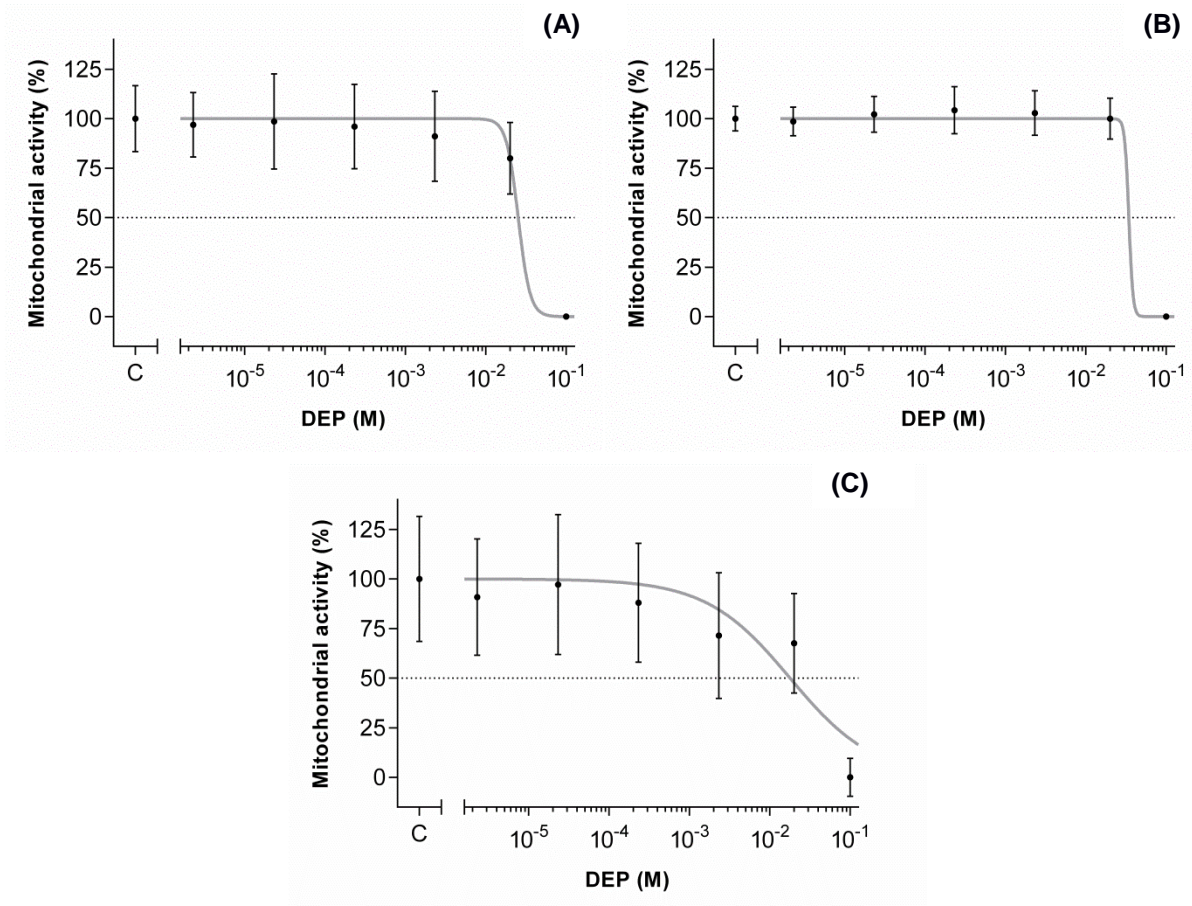


**Figure 15.** Mitochondrial activity of hepatocytes exposed to DEP at the **(A)** first replicate **(B)** second replicate and **(C)** third replicate (% of control; mean  $\pm$  standard deviation; C: control).

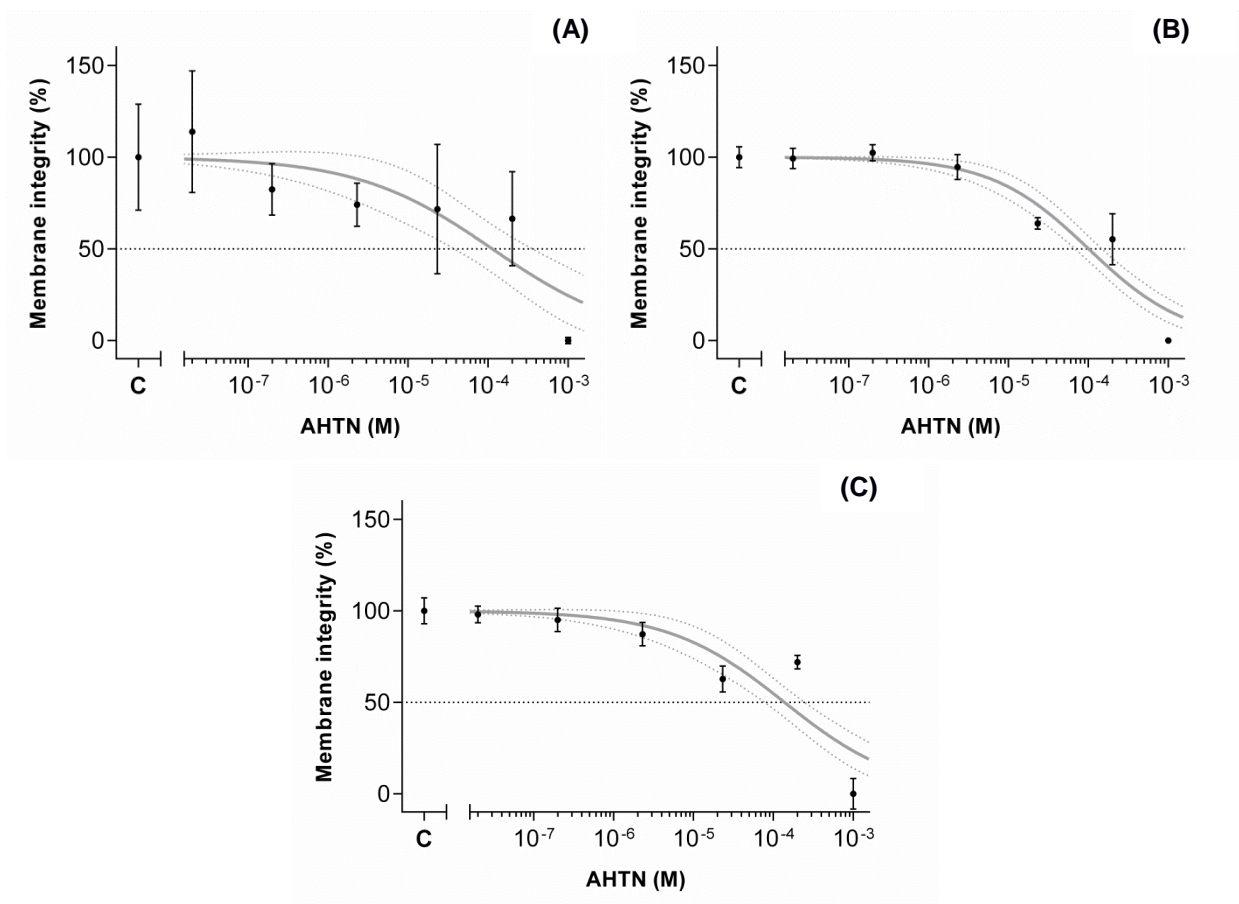


**Figure 16.** Membrane integrity of hepatocytes exposed to AHTN at the **(A)** first replicate **(B)** second replicate and **(C)** third replicate (% of control; mean  $\pm$  standard deviation; dotted lines: 95% confidence interval; C: control).

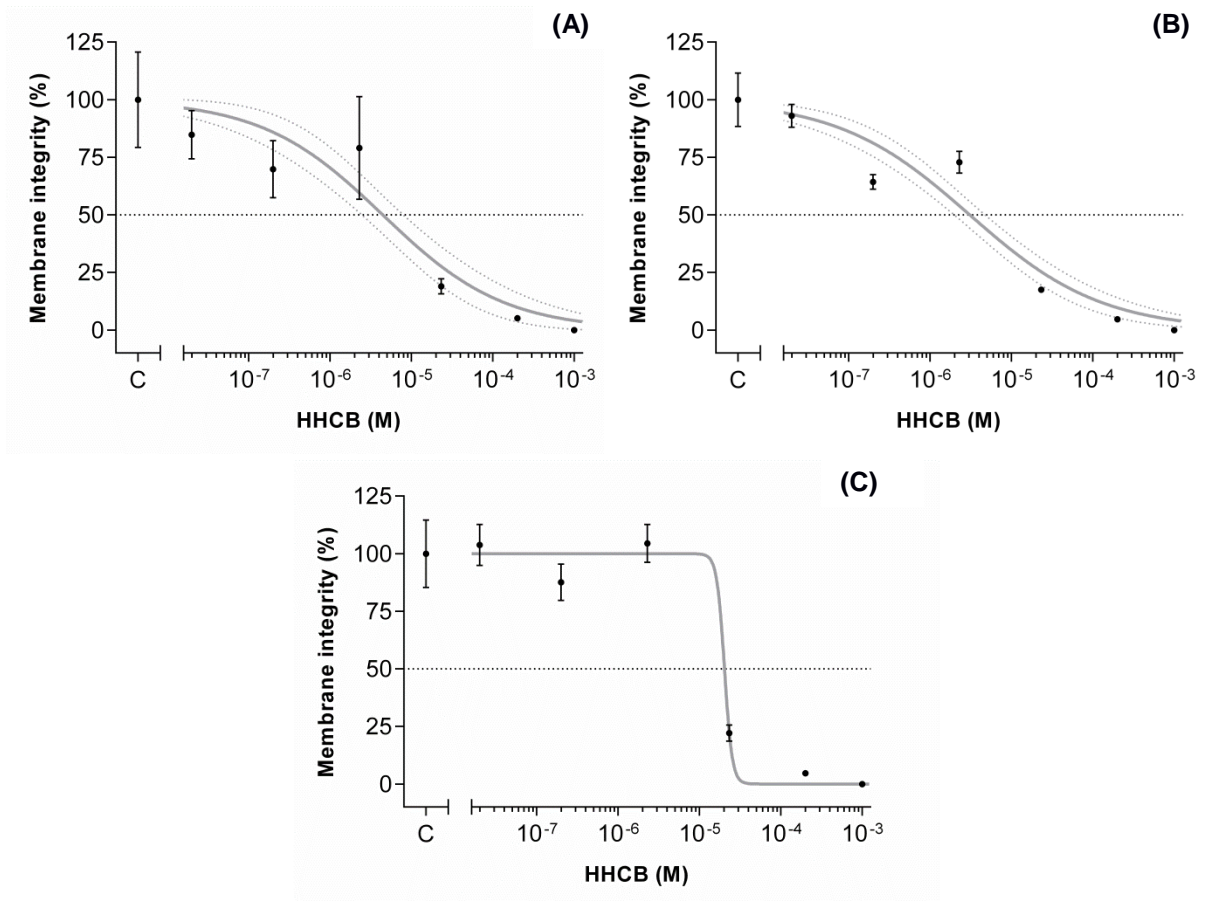


**Figure 17.** Membrane integrity of hepatocytes exposed to HHCB at the **(A)** first replicate **(B)** second replicate and **(C)** third replicate (% of control; mean  $\pm$  standard deviation; dotted lines: 95% confidence interval; C: control).

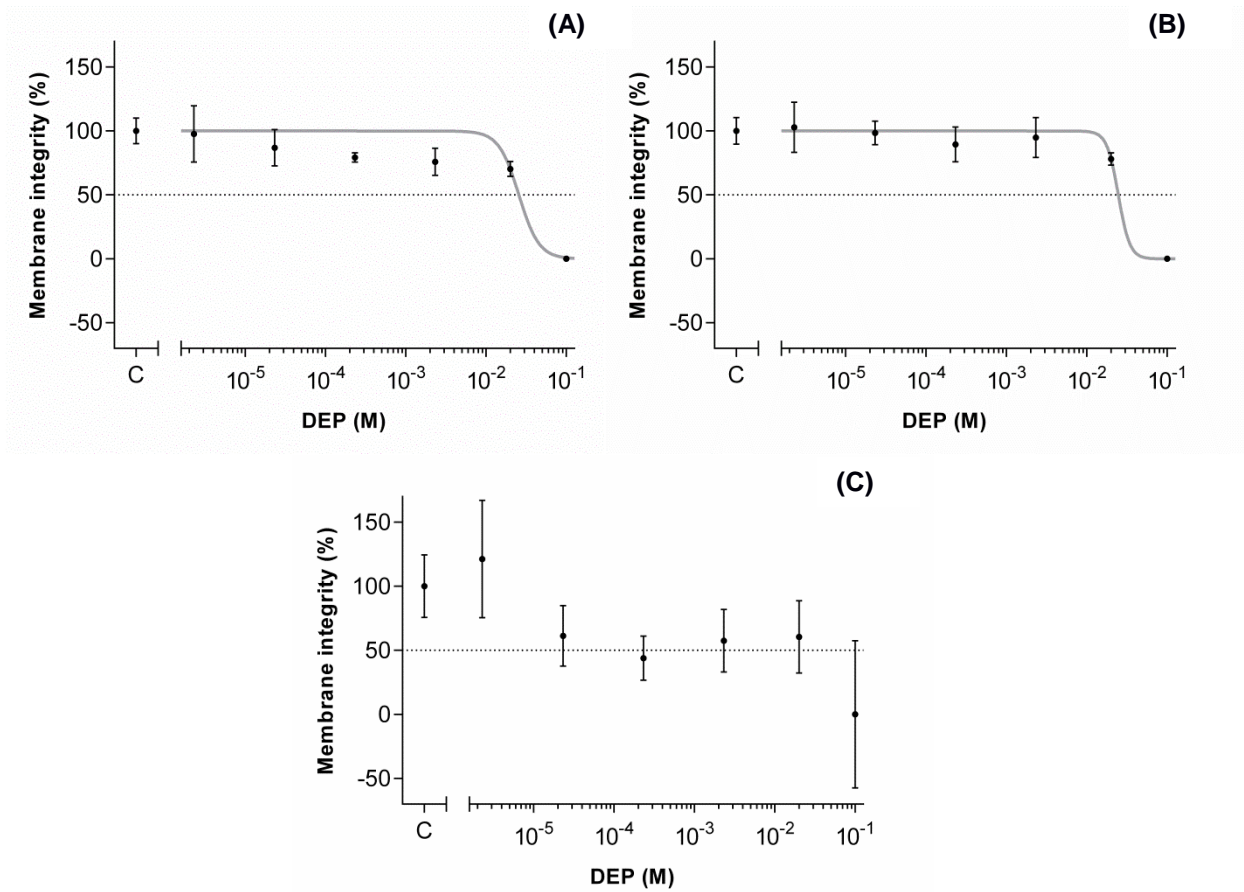


**Figure 18.** Membrane integrity of hepatocytes exposed to DEP at the (A) first replicate (B) second replicate and (C) third replicate (% of control; mean ± standard deviation; C: control).

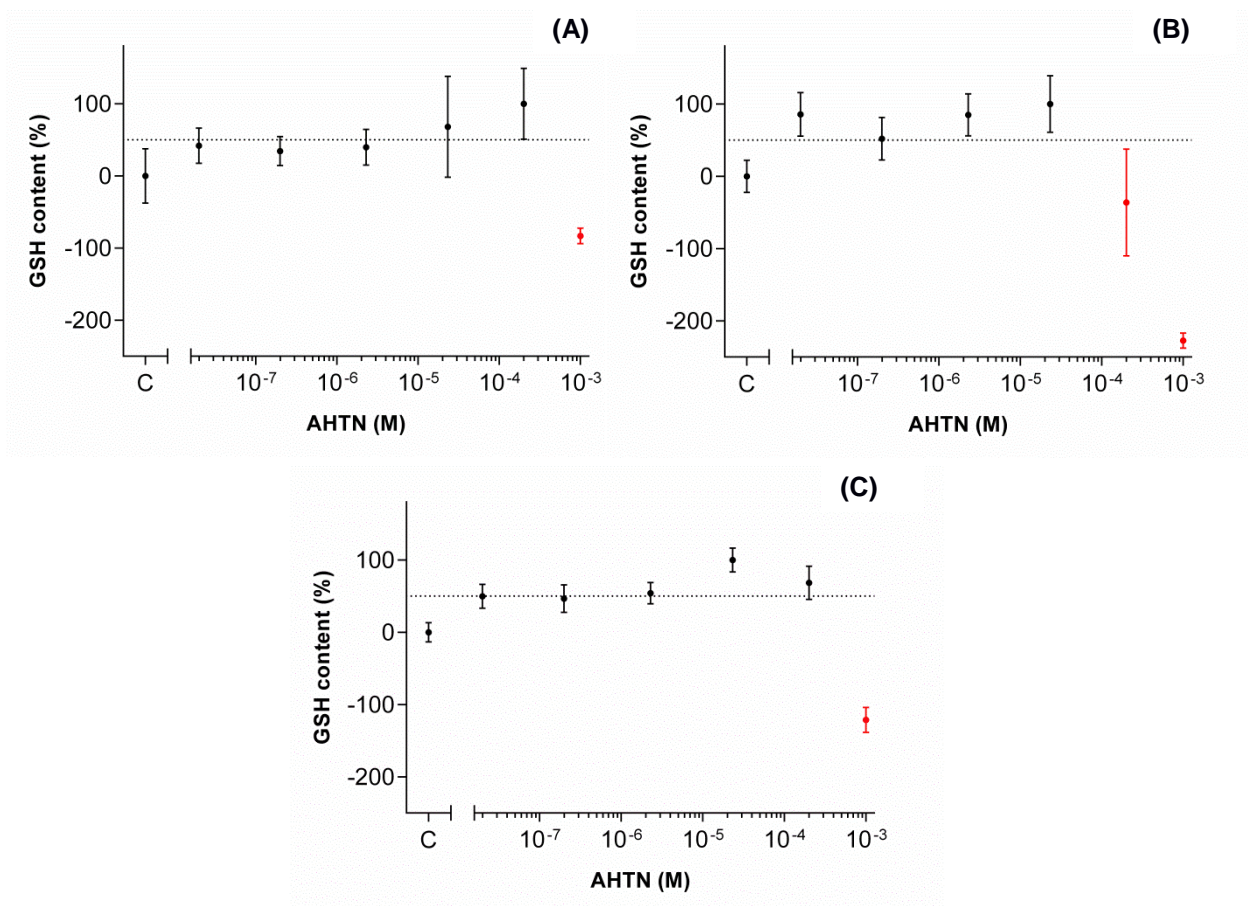


**Figure 19.** GSH content of hepatocytes exposed to AHTN at the **(A)** first replicate **(B)** second replicate and **(C)** third replicate (% of control; mean  $\pm$  standard deviation; C: control; red error bars: concentrations excluded from the graphical analysis).

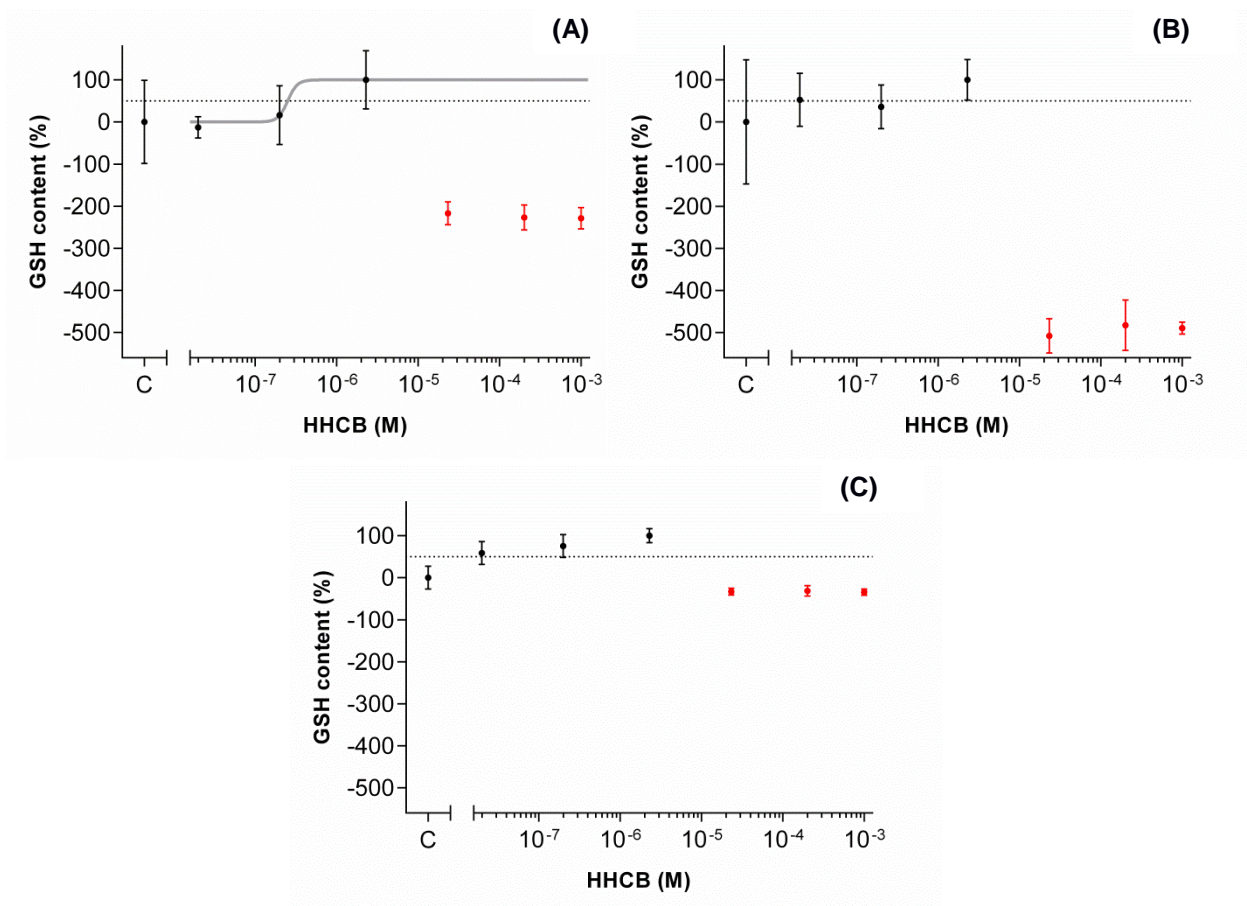


**Figure 20.** GSH content of hepatocytes exposed to HHCB at the **(A)** first replicate **(B)** second replicate and **(C)** third replicate (% of control; mean  $\pm$  standard deviation; C: control; red error bars: concentrations excluded from the non-linear regression curve fit and graphical analysis).

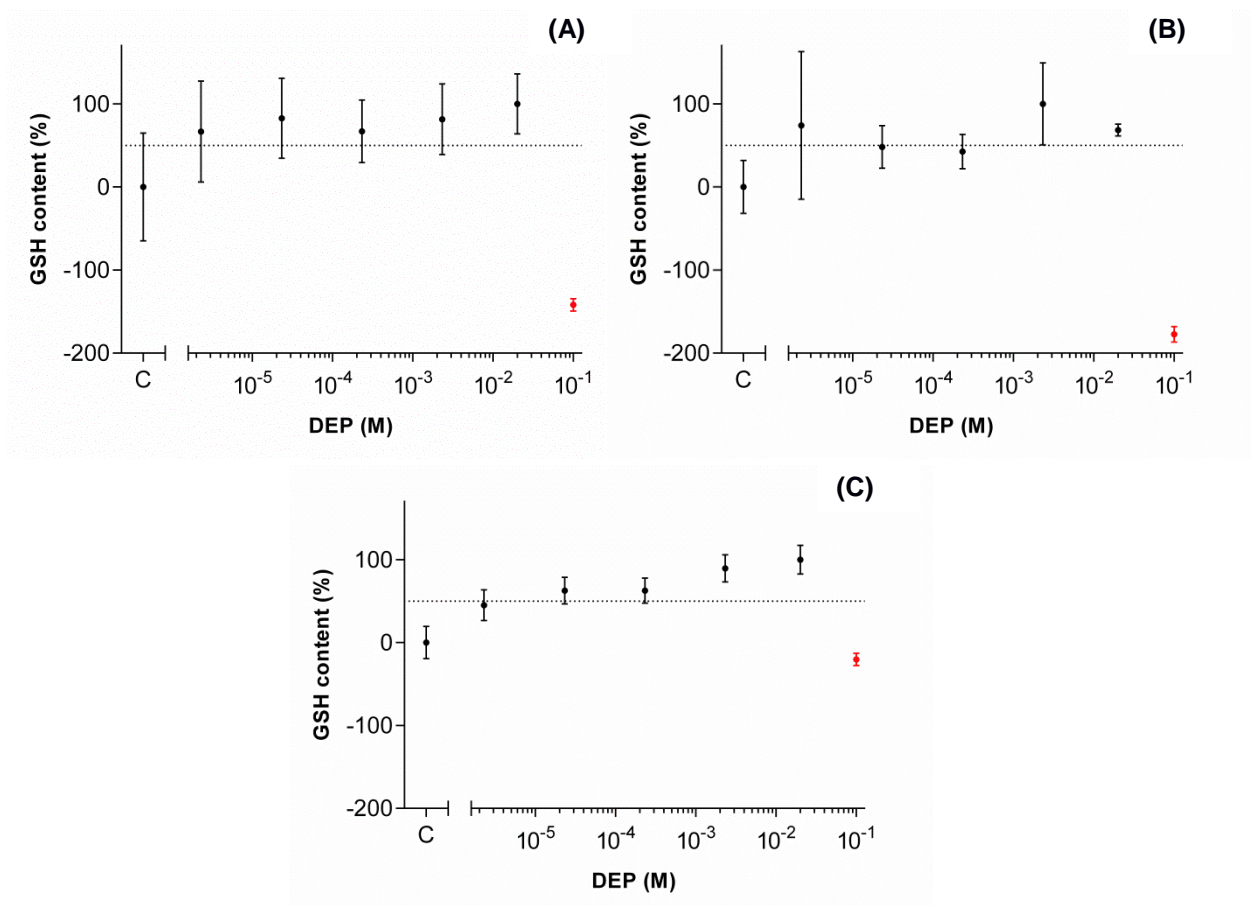


**Figure 21.** GSH content of hepatocytes exposed to DEP at the **(A)** first replicate **(B)** second replicate and **(C)** third replicate (% of control; mean ± standard deviation; C: control; red error bars: concentrations excluded from the graphical analysis).



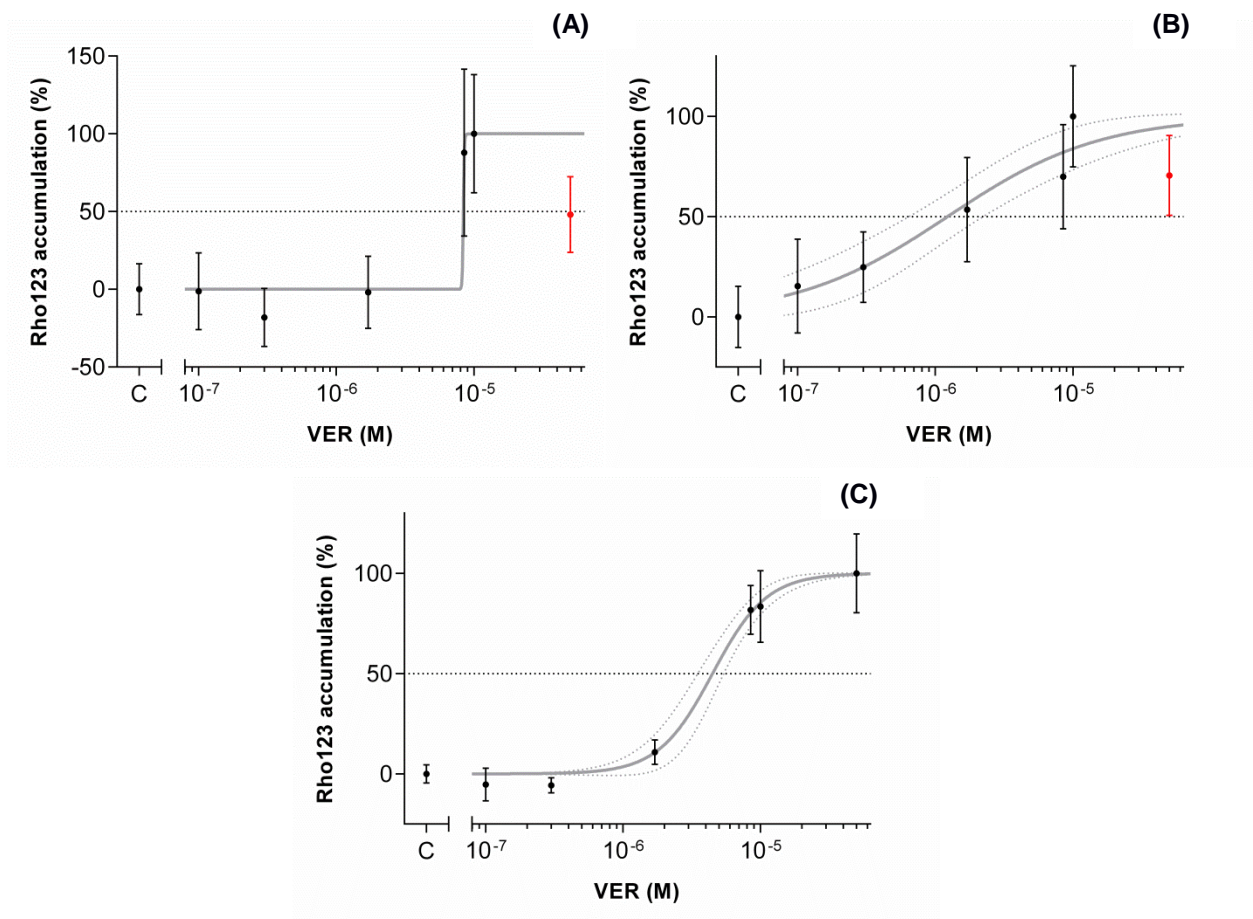


**Figure 22.** Rho123 accumulation on hepatocytes exposed to the inhibitor VER at the **(A)** first replicate **(B)** second replicate and **(C)** third replicate (% of control; mean  $\pm$  standard deviation; dotted lines: 95% confidence interval; C: control; red error bars: concentrations excluded from the non-linear regression curve fit).

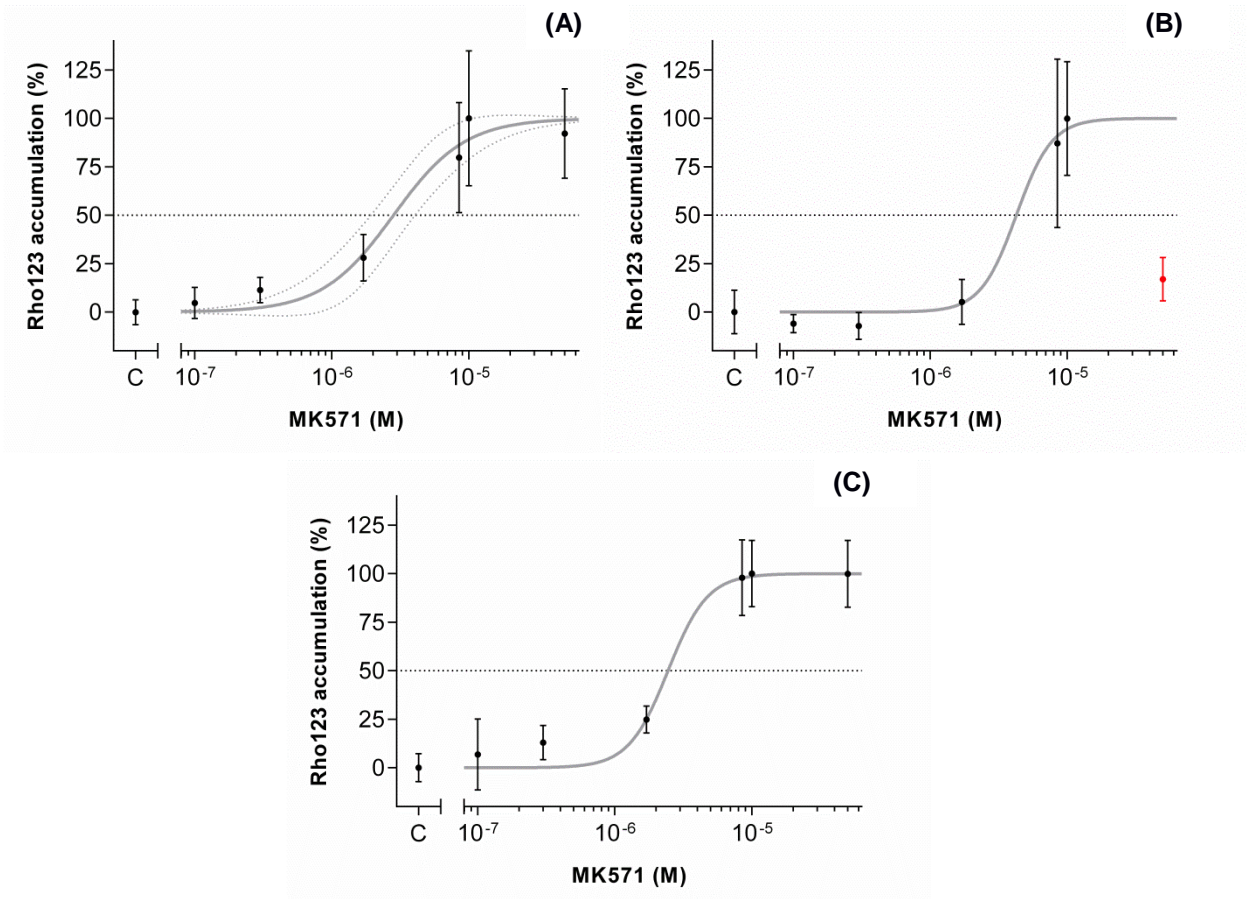


**Figure 23.** Rho123 accumulation on hepatocytes exposed to the inhibitor MK571 at the **(A)** first replicate **(B)** second replicate and **(C)** third replicate (% of control; mean  $\pm$  standard deviation; dotted lines: 95% confidence interval; C: control; red error bars: concentrations excluded from the non-linear regression curve fit).

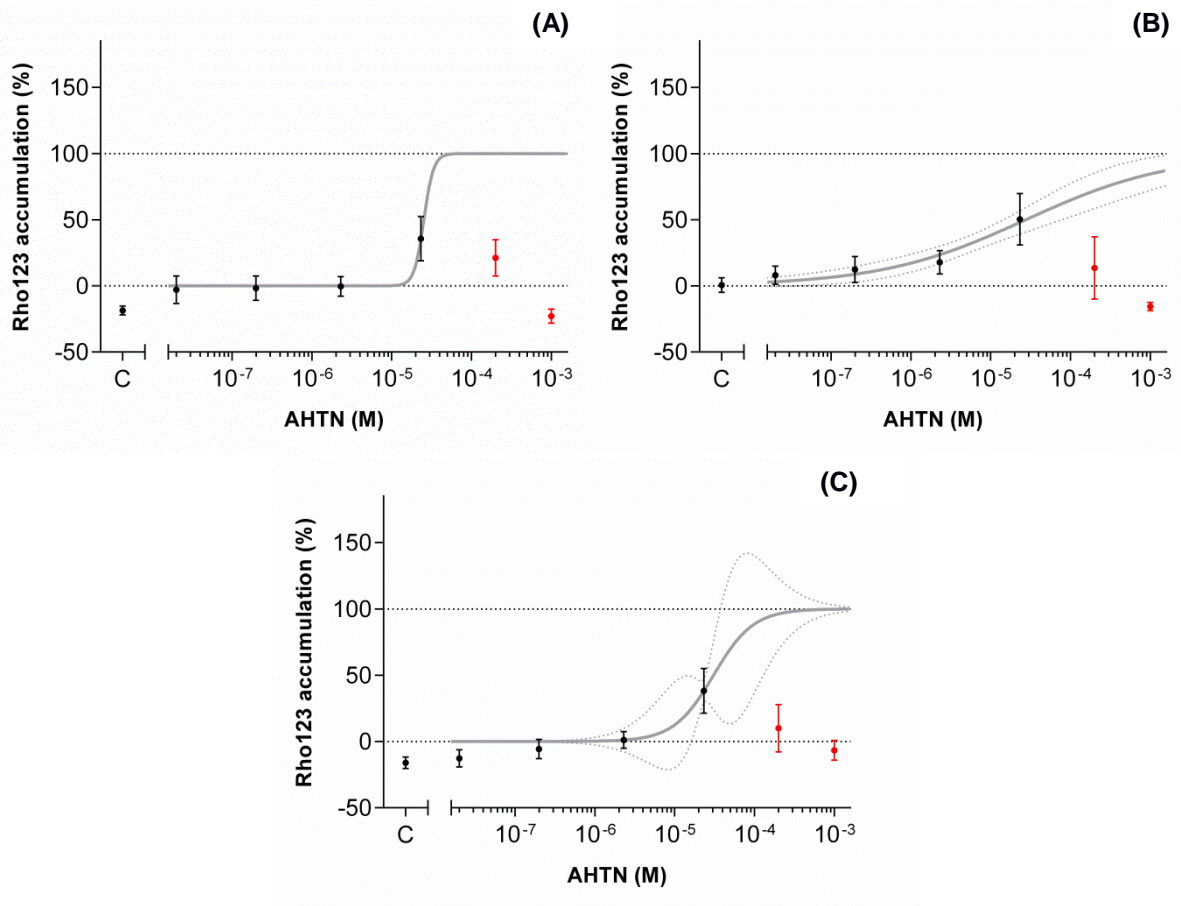


**Figure 24.** Rho123 accumulation on hepatocytes exposed to AHTN at the **(A)** first replicate **(B)** second replicate and **(C)** third replicate (% of MK571; mean  $\pm$  standard deviation; dotted lines: 95% confidence interval; C: control; red error bars: concentrations excluded from the non-linear regression curve fit).

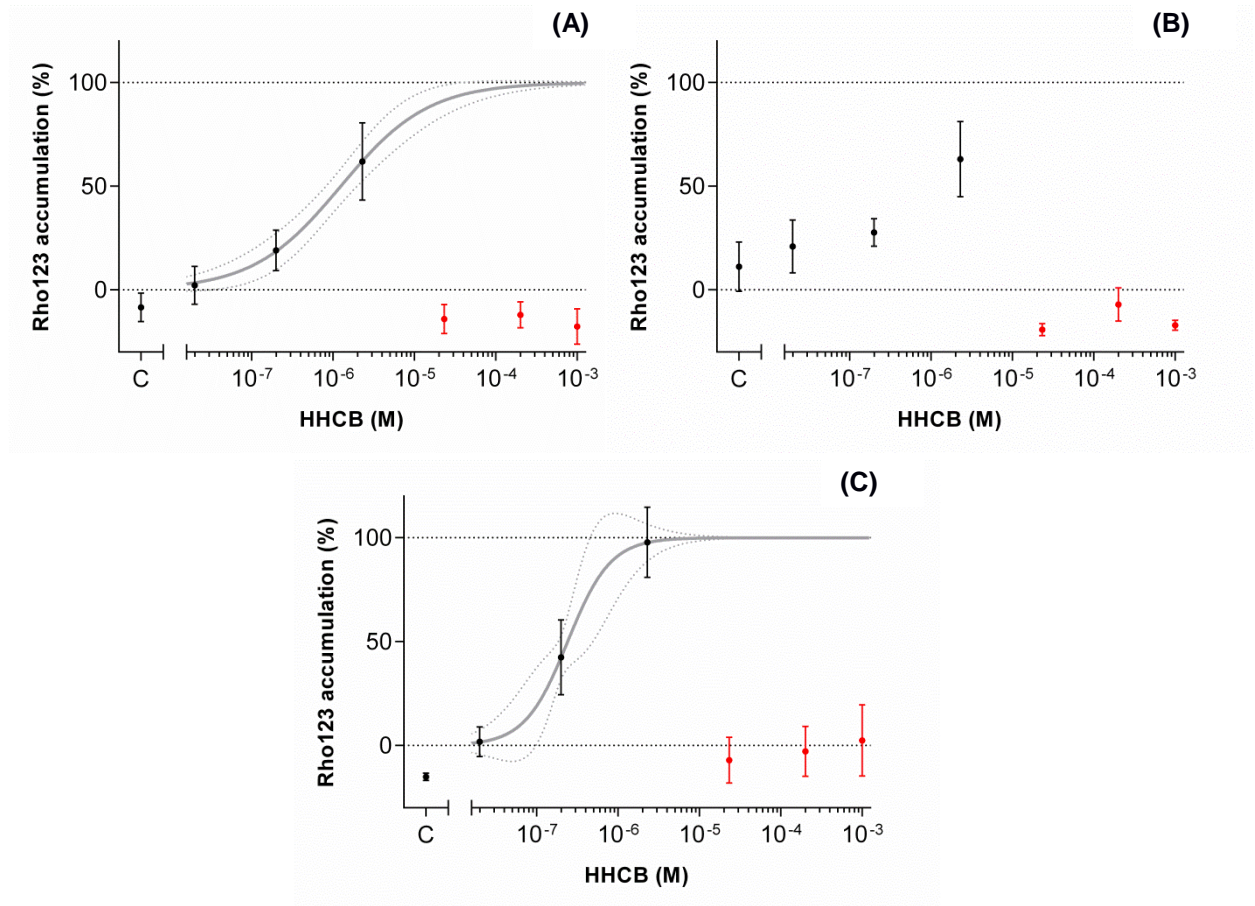


**Figure 25.** Rho123 accumulation on hepatocytes exposed to HHCB at the **(A)** first replicate **(B)** second replicate and **(C)** third replicate (% of MK571; mean  $\pm$  standard deviation; dotted lines: 95% confidence interval; C: control; red error bars: concentrations excluded from the non-linear regression curve fit).

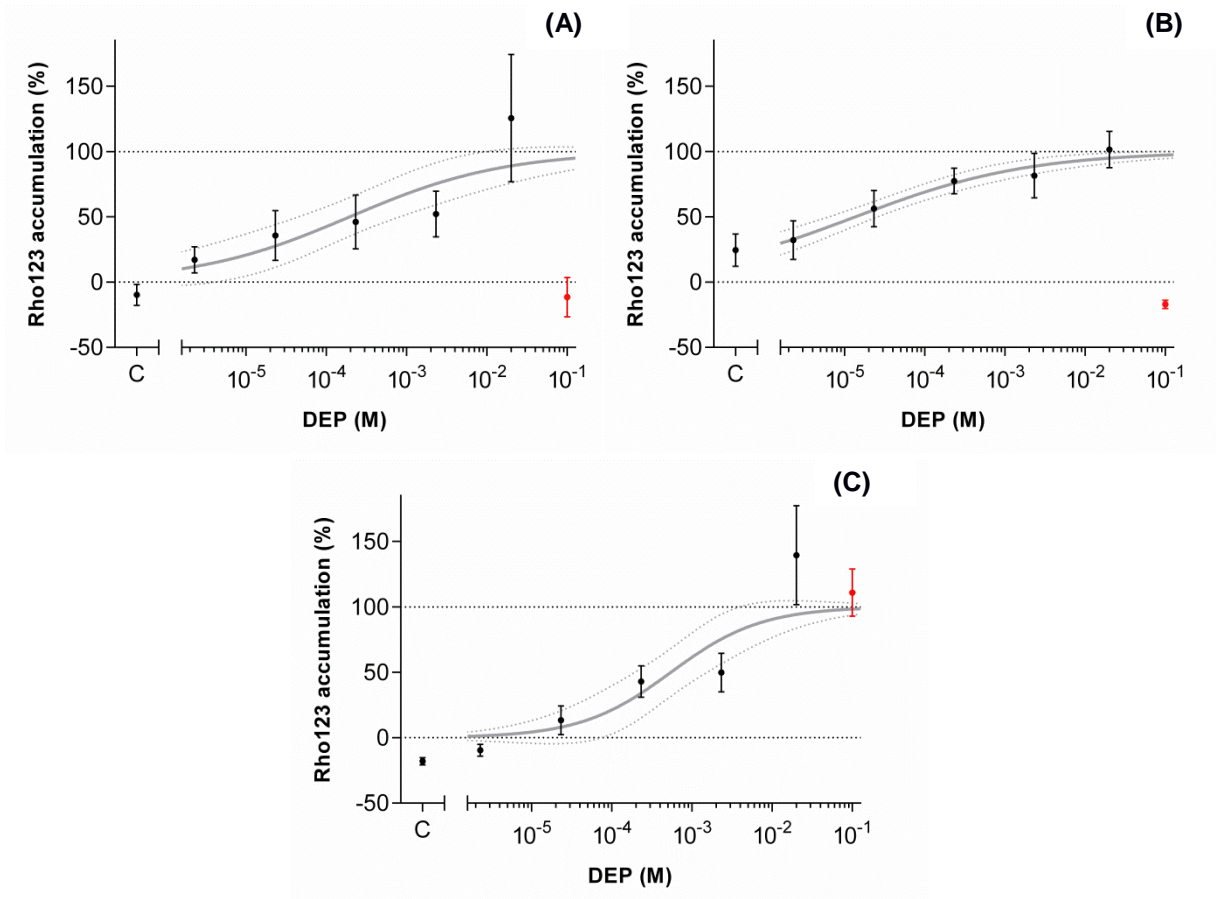


**Figure 26.** Rho123 accumulation on hepatocytes exposed to DEP at the **(A)** first replicate **(B)** second replicate and **(C)** third replicate (% of MK571; mean  $\pm$  standard deviation; dotted lines: 95% confidence interval; C: control; red error bars: concentrations excluded from the non-linear regression curve fit).

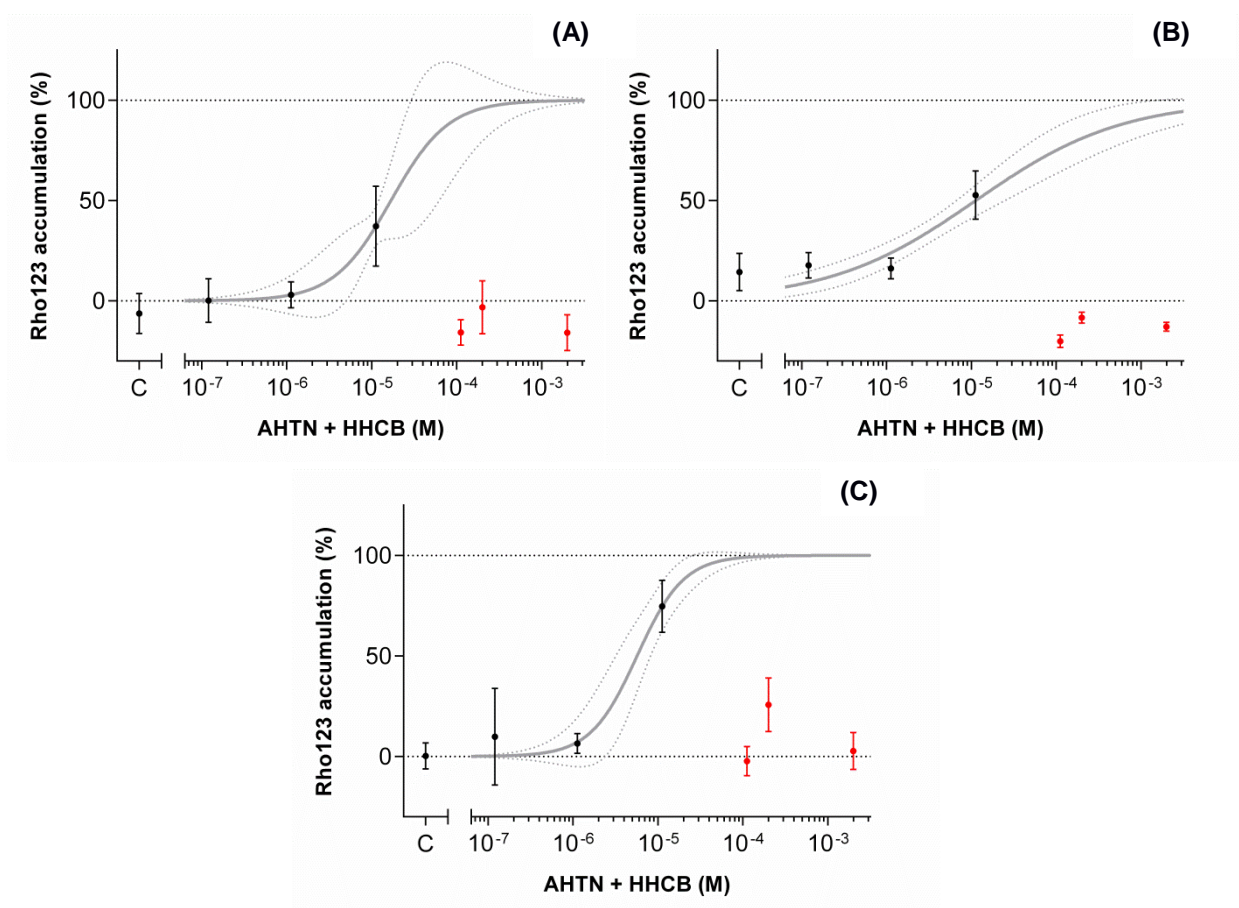


**Figure 27.** Rho123 accumulation on hepatocytes exposed to a mixture of AHTN and HHCB at the **(A)** first replicate **(B)** second replicate and **(C)** third replicate (% of MK571; mean  $\pm$  standard deviation; dotted lines: 95% confidence interval; C: control; red error bars: concentrations excluded from the non-linear regression curve fit).

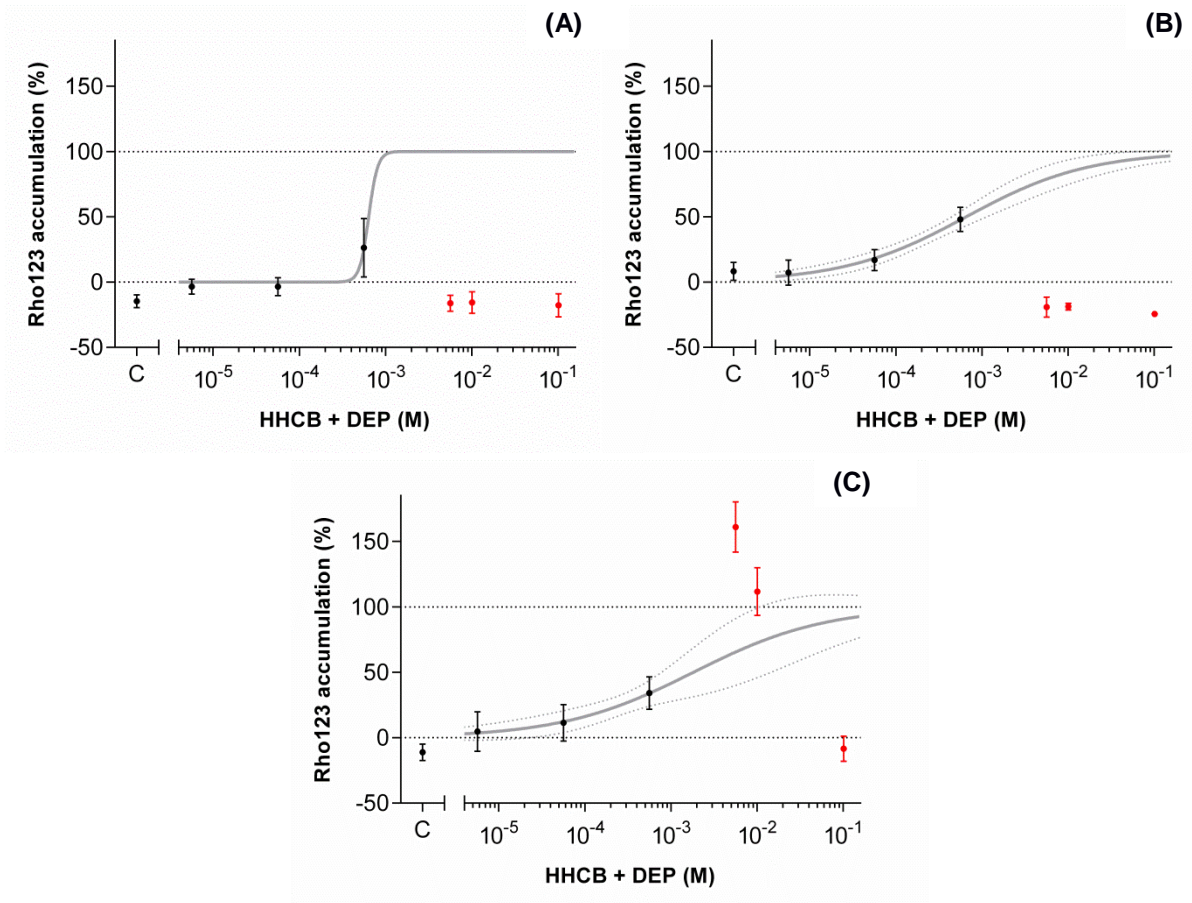


**Figure 28.** Rho123 accumulation on hepatocytes exposed to a mixture of HHCB and DEP at the **(A)** first replicate **(B)** second replicate and **(C)** third replicate (% of MK571; mean  $\pm$  standard deviation; dotted lines: 95% confidence interval; C: control; red error bars: concentrations excluded from the non-linear regression curve fit).